CONTRACTOR REPORT BRL-CR-681

BRL

INTERFEROMETRIC OPTICAL HIGH PRESSURE SENSOR

THOMAS R. STEELE
PRINCIPAL INVESTIGATOR
LIGHTWAVE ELECTRONICS CORPORATION

JANUARY 1992

U.S. ARMY LABORATORY COMMAND

BALLISTIC RESEARCH LABORATORY
ABERDEEN PROVING GROUND, MARYLAND

NOTICES

Destroy this report when it is no longer needed. DO NOT return it to the originator.

Additional copies of this report may be obtained from the National Technical Information Service, U.S. Department of Commerce, 5285 Port Royal Road, Springfield, VA 22161.

The findings of this report are not to be construed as an official Department of the Army position, unless so designated by other authorized documents.

The use of trade names or manufacturers' names in this report does not constitute indorsement of any commercial product.

REPORT DOCUMENTATION PAGE

Form Approved
OMB No. 0704-0188

1. AGENCY USE ONLY (Leave blank)	2. REPORT DATE	3. REPORT TYPE AND DATES COVERED
	January 1992	Final, December 1988–February 1990

4. TITLE AND SUBTITLE

Interferometric Optical High Pressure Sensor

5. FUNDING NUMBERS

DAAA15-38-C-0053

6. AUTHOR(S)

Thomas R. Steele, Principal Investigator

7. PERFORMING ORGANIZATION NAME(S) AND ADDRESS(ES)

LIGHTWAVE Electronics Corporation
1161 San Antonio Road
Mountain View, CA 94043

8. PERFORMING ORGANIZATION REPORT NUMBER

9. SPONSORING / MONITORING AGENCY NAME(S) AND ADDRESS(ES)

U.S. Army Ballistic Research Laboratory
ATTN: SLCBR-DD-T
Aberdeen Proving Ground, MD 21005-5066

10. SPONSORING / MONITORING AGENCY REPORT NUMBER

BRL–CR–681

11. SUPPLEMENTARY NOTES

Technical POC: U.S. Army Ballistic Research Laboratory, ATTN: SLCBR-IB-I (R. Beyer), Aberdeen Proving Ground, MD, 21005-5066

12a. DISTRIBUTION / AVAILABILITY STATEMENT

Approved for public release; distribution is unlimited.

12b. DISTRIBUTION CODE

13. ABSTRACT *(Maximum 200 words)*

A high pressure sensor has been built and tested based on measuring the compression of an optical etalon and recording the resulting fringe shifts. A birefringent sapphire etalon has been used along with polarized light to make the etalon function as a dual-thickness device; the result is to remove the ambiguity of direction of pressure change that results from a single etalon device. Details of the pressure head design, pressure sealing, and system evaluation are presented. Design goals of better than 5,000 psi accuracy over a range up to 150,000 psi with time resolution better than 0.1 ms are projected to be met from preliminary tests.

14. SUBJECT TERMS

pressure; sensor; optics; etalon; electromagnetic interference

15. NUMBER OF PAGES

62

16. PRICE CODE

17. SECURITY CLASSIFICATION OF REPORT	18. SECURITY CLASSIFICATION OF THIS PAGE	19. SECURITY CLASSIFICATION OF ABSTRACT	20. LIMITATION OF ABSTRACT
UNCLASSIFIED	UNCLASSIFIED	UNCLASSIFIED	SAR

INTENTIONALLY LEFT BLANK.

TABLE OF CONTENTS

LIST OF FIGURES

INTENTIONALLY LEFT BLANK.

1. INTRODUCTION

This report describes research to investigate the measurement of high pressure transient events under adverse conditions, such as in a gun chamber during weapon firing, using an optical system that is immune to electromagnetic interference. It is a summary of work performed by LIGHTWAVE Electronics Corp., under a Phase II contract of the Army SBIR program for the U.S. Army Ballistic Research Laboratory (BRL) at Aberdeen Proving Ground (APG), MD.

The aim of this research was to perform an exploratory development effort to investigate an optical measurement system that would provide a means of measuring pressures in physically or electrically harsh environments. It was desired to develop a compact optical pressure transducer that could be located remotely using an optical fiber to connect the sensor to the optical source and detector. The sensor would ideally be minimally intrusive, durable, require low power, and have fast response, wide range, good sensitivity, and immunity to electromagnetic interference. A sensor system with this combination of properties is not presently available. It is expected that such a measurement system would be useful to the Army for making real-time measurements of pressure transients during weapon development and ammunition testing programs. In particular, it would be of great use in the testing of electrothermal guns presently under development by the Army; with currently available electrical sensors, difficulties are encountered when testing these guns due to the intense electromagnetic pulse produced when they are fired, which disturbs electrical sensors. Many industrial situations also require the measurement of high pressures in the range that can be covered by this system.

Measurements of pressure inside large caliber weapons are critical for establishing the balance between crew safety and combat effectiveness. A 2% error in chamber pressure measurement can result in a 3% change in weight, a 4% change in effective range, and a 6% change in fatigue life. For electrical pressure transducers, it is possible for a given type of transducer to consistently distinguish dynamic pressure variations as small as 0.2%; yet different models of pressure transducers can disagree by as much as 2% (Walton 1983).

LIGHTWAVE Electronics performed research under an Army SBIR Phase I program from July 1987 to January 1988 that demonstrated the feasibility of developing an optical pressure measurement system, justifying the continuation of the work in a Phase II program in order to explore the development of such a system. The results of the Phase I effort are described in the Phase I Final Report.

2. OPTICAL MEASUREMENTS

Although numerous optical measurement techniques such as classical interferometry have been used for many years, the availability of high quality optical fibers has broadened the scope of the field considerably over the last two decades. This is due mostly to the high efficiency and enormous flexibility that optical fibers provide in the transport of optical beams. In addition, optical fibers may serve as the sensing elements for a transducer, thereby permitting a variety of new measurements to be made, often with much higher sensitivity. Indeed, interferometric sensors based on single mode fiber provide the highest sensitivity to many measurands (Kersey, Giallorenzi, and Dandridge 1989). Besides their good sensitivity, fiber optic sensors also have the advantages of providing sensors of small size that are not only immune to electromagnetic interference but are completely electrically isolated. As a result, they are generally an attractive alternative in hazardous or explosive environments, in high temperature or high electromagnetic field environments, and for in vivo medical applications. The parallel development of low attenuation optical fibers and lasers and compact semiconductor sources and detectors has now led to the proliferation of innovative optical sensor concepts which seem to be limited only by the ingenuity of researchers. Many designs have been demonstrated for the measurement of temperature, pressure, electric and magnetic fields, position, strain, acceleration, rotation (gyroscopes), acoustic signals (hydrophones), fluid level, flow, radiation, and chemical species (Giallorenzi et al. 1982).

Sensors based on fiber optics may be broadly classified into intensity sensors which have an output determined directly by the detected optical power level or interferometric sensors which have an output determined by the phase of the detected optical signal. Intensity sensors generally have moderate sensitivity but are inexpensive and easy to implement, while interferometric sensors tend to have high sensitivity but are rather sophisticated. Fiber optic sensors may also be classified as extrinsic sensors, in which the transducer is distinct from

the fiber, which acts simply as a "lightpipe," or as intrinsic sensors, in which a section of fiber acts directly as the transducer. It is our belief that the extreme environment encountered in gun chambers precludes the use of intrinsic fiber sensors due to the incompatibility of this environment with the somewhat fragile nature of silica fibers. In addition, intrinsic sensors generally suffer from the drawback that they are sensitive to many environmental parameters, so that it is frequently difficult to isolate the single parameter of interest.

3. SYSTEM OVERVIEW

Here we have explored the development of an extrinsic interferometric optical high pressure sensor system. This approach is based on the use of a compact solid Fabry-Perot etalon as the transducer (Born and Wolf 1975). An etalon is an interferometer composed of two partially reflective surfaces which flank an optically transmissive region to form an optical cavity. The reflection from or transmission through such an interferometer varies with the following parameters:

(1) the wavelength of the light,
(2) the angle of incidence of the light upon the etalon,
(3) the reflectivity of the etalon surfaces,
(4) the losses in the etalon cavity,
(5) the optical path length of the transmissive region.

In this application, it is the pressure dependence of the last parameter, the optical path length, that is exploited in order to utilize an etalon as a pressure sensor. The other four parameters should remain essentially unchanged; any variations in them lead to inaccuracies in the measurement.

The interference signal from the etalon sensor could be monitored either using the light reflected from the face on which the laser beam is incident or else using the light transmitted through the etalon (see Figure 1). This application requires monitoring of the reflected signal since it is not possible to access the transmitted signal in a gun chamber environment.

The configuration of the pressure measurement system (utilizing an etalon as the transducer) is as follows. Light from a laser source is coupled into a single mode optical fiber

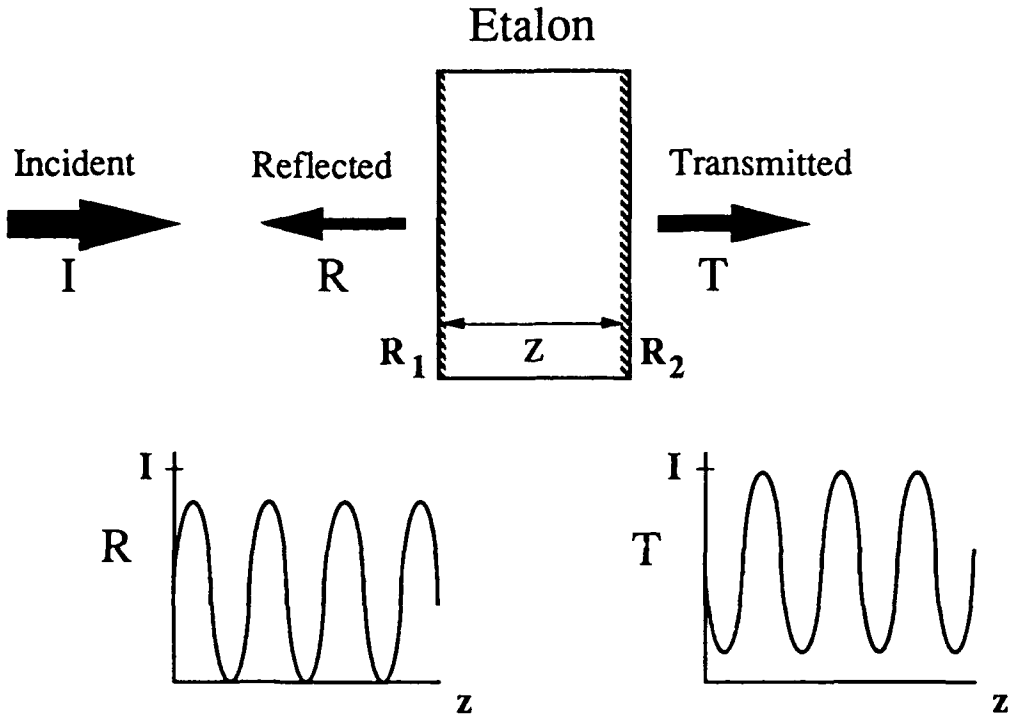

Figure 1. Schematic View of an Etalon Illustrating the Principle of the Measurement Technique. Two Interference Signals Can Potentially Be Detected From an Etalon—the Reflected Signal (R) and the Transmitted Signal (T). These Signals Would Vary as Shown as the Optical Path Length Changes.

which conveys it to an etalon located at the far end of the fiber. The reflected signal from the etalon is coupled back into the same fiber, which conveys it back to the input end where a beam splitter reflects a portion of it to a detector module. The strength of the received signal depends on the distance between the two etalon surfaces. So pressure variations that produce changes in this distance can be detected by monitoring the returned signal. The essential components of such a system are shown schematically in Figure 2. The feasibility of this system was demonstrated during the Phase I portion of this program.

3.1 Objectives. The goal of this exploratory development effort was to construct and test an integrated high pressure measurement system useful in harsh environments, such as encountered in weapon development and ammunition testing, and particularly in environments where there is a large amount of electromagnetic interference present, such as the testing of electrothermal guns. Consequently, the system is designed and optimized for measuring brief impulse events with pressures in the range encountered in gun chambers on a short time

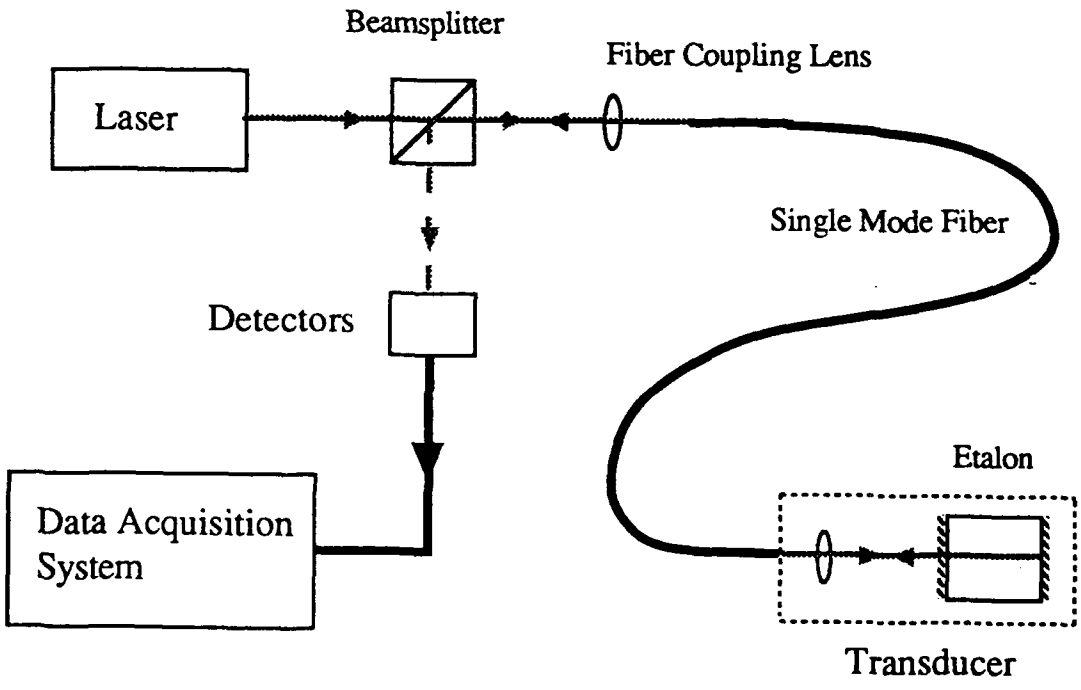

Figure 2. The Layout of the Basic Components of the High Pressure Measurement System.

scale of the order of milliseconds. The specification goals for the desired pressure measurement system are the following:

(1) pressure range: 0 to 150,000 psi,
(2) accuracy: 5,000 psi,
(3) resolution: 1,000 psi,
(4) temporal resolution: 0.1 millisecond.

In addition, the system should incorporate an all-optical sensor and data link that would be immune to electromagnetic interference, and the transducer should have an external design compatible with the 6211-type transducer manufactured by Kistler Instruments, NY, in order to be compatible with the testing equipment at APG that is already adapted for the use of Kistler 6211 pressure transducers.

Since in this application, the etalon directly experiences the high pressures produced by the firing of large caliber guns (up to 150,000 psi), it is necessary to form the etalon from a

solid slab of highly durable optical material that can withstand such high pressures; yet is compressed by a detectable amount. In this system, the etalon consists of a 5-mm-thick piece of sapphire with partially reflective coatings applied to its surfaces and compression of the sapphire produces interference fringes that can be detected and used to yield a pressure measurement. A detailed discussion of a practical transducer design is presented.

3.2 Transducer Sensitivity. The material chosen for the fabrication of the etalon transducer was sapphire. It is a well-known material which has the properties required here (Crystal Systems Inc. 1990). Optical quality man-made sapphire is readily available and moderately priced. It is an extremely hard material (Moh hardness = 9 by definition), is durable and chemically inert, and has a high melting point (2,053° C). It has high internal transmittance over a wide range of wavelengths (λ = 0.15–6.0 μm) and has great strength, so that it is a popular choice for thin optical windows. In addition, it has a low susceptibility to radiation damage, having proved to be resistant to radiation browning and luminescence in a reactor environment.

Sapphire is single crystal aluminum oxide ($Al_2 O_3$). Because of its hexagonal crystalline structure, it exhibits anisotropy in many optical and physical properties. The exact characteristics of an optical component made from sapphire depend on the orientation of the optic axis (c -axis) relative to the surface of the component. In particular, the anisotropy leads to sapphire being birefringent, so that the refractive index differs by 0.008 between light travelling along the optic axis and light travelling perpendicular to it. This property of sapphire is useful for the application being considered here, as will be described.

We selected an etalon thickness of 5 mm to obtain a transducer of sufficient thickness that could withstand the high pressures encountered in this application. The sensitivity of an etalon to pressure changes may be computed as follows. The optical thickness of the etalon (L) is

$$L = n\, z,$$

where

n = optical index of refraction,

z = physical thickness of etalon,

and both of these parameters vary with pressure. The change in optical path length with pressure is given by the following:

$$\frac{\partial L}{\partial p} = n\frac{\partial z}{\partial p} + z\frac{\partial n}{\partial p}. \tag{1}$$

The degree to which sapphire is compressed linearly by the application of a pressure from one direction is given by the following compressive modulus (Crystal Systems Inc. 1990):

$$\begin{aligned} z\frac{\partial p}{\partial z} &= -55 \times 10^6\, psi \\ \Rightarrow \frac{\partial z}{\partial p} &= \frac{-z}{55 \times 10^6\, psi}. \end{aligned} \tag{2}$$

Consequently, when a sapphire etalon is compressed by 150,000 psi (the maximum pressure that the transducer is expected to measure), its fractional change in length would be 0.0027. For a 5-mm-thick etalon, the physical decrease in thickness would thus be 14 μm.

The index of refraction of sapphire at $\lambda = 1.06$ μm (the wavelength of the source used here) is $n = 1.75$, varying with orientation since the material is slightly birefringent. The change in index of refraction under isotropic (hydrostatic) compression for sapphire is

$$\rho\frac{\partial n}{\partial \rho} \approx 0.25, \tag{3}$$

varying slightly with crystal orientation (Pinnow 1970). The isotropic compressibility (the inverse of the bulk modulus) of sapphire is

$$\frac{1}{\rho}\frac{\partial \rho}{\partial p} = \frac{1}{35 \times 10^6\, psi}. \tag{4}$$

Thus,

$$\frac{\partial n}{\partial p} = \rho \frac{\partial n}{\partial \rho} \times \frac{1}{\rho} \frac{\partial \rho}{\partial p} = \frac{0.25}{35 \times 10^6 \, psi}. \tag{5}$$

Consequently, for a pressure change of 150,000 psi, the increase in index of refraction would be 0.0011.

Using these values, the change in optical path length with pressure is

$$\frac{\partial L}{\partial p} = -2.5 \times 10^{-8} z \quad psi^{-1} \quad \text{(z in meters)}. \tag{6}$$

In this case, the two terms in Equation 1 enter with opposite signs so that the two separate effects partially cancel. This arises since the thickness decreases with increasing pressure, but the index of refraction increases with pressure for sapphire (most, but not all, materials show this behavior; some exhibit a decrease in index of refraction with increasing pressure).

This may be reexpressed in terms of the number of fringes observed in the interference pattern of the etalon; for $\lambda = 1.06$ μm,

$$\frac{\partial N}{\partial p} = \frac{2}{\lambda} \left| \frac{\partial L}{\partial p} \right| = 4.7 \times 10^{-2} z \quad \text{fringe/psi} \quad \text{(z in meters)}. \tag{7}$$

So for the etalon thickness used (z = 5 mm), the pressure change corresponding to one fringe shift is expected to be about 4,300 psi. And for the full pressure range of 150,000 psi, we expect to observe about 35 fringe shifts which permit accurate detection of the pressure change.

Instead of simply counting fringes to yield discrete pressure readings, the resolution of the transducer can be improved by carefully monitoring the details of the interference pattern.

Also, because the fringe spacing is linearly dependent on the etalon thickness, the resolution of the transducer can be tuned simply by increasing or decreasing its thickness.

Of course, the refractive index and thickness of the etalon also vary with temperature. The change in optical path length with temperature is given by the following:

$$\frac{\partial L}{\partial T} = n\frac{\partial z}{\partial T} + z\frac{\partial n}{\partial T}. \tag{8}$$

The coefficient of thermal expansion of sapphire (for 0–500° C) (Melles Griot Corp. 1988),

$$\frac{1}{z}\frac{\partial z}{\partial T} \approx 7.7 \times 10^{-6}/°C, \tag{9}$$

is typical for a hard optical crystal. The temperature coefficient for index of refraction (Gray 1982) is

$$\frac{\partial n}{\partial T} \approx 13 \times 10^{-6}/°C. \tag{10}$$

Using these values, the change in optical path length with temperature is

$$\frac{\partial L}{\partial T} = 27 \times 10^{-6}\, z\ /°C \quad (\text{z in meters}). \tag{11}$$

This may be reexpressed in terms of the number of fringes observed in the interference pattern of the etalon; for $\lambda = 1.06\ \mu m$,

$$\frac{\partial N}{\partial T} = \frac{2}{\lambda}\frac{\partial L}{\partial T} = 51\, z\ \text{fringe}/°C \quad (\text{z in meters}). \tag{12}$$

Consequently, for the etalon thickness used (z = 5 mm), the fringe shift per °C is predicted to be 0.25 (i.e., a temperature change of 4° C leads to the observed interference pattern

shifting by one fringe). Thus, if thermal effects are to be ignored, the etalon must be stable to about 1° C during the period of the pressure measurement. So to make a sensible pressure measurement, the etalon must be isolated from the immediate effects of the temperature rise associated with the pressure transient being measured. Since the etalon has dimensions of the order of millimeters, the thermal conduction time through the sapphire is about a second. This greatly exceeds the time for the pressure propagation (the acoustic transit time), which is a fraction of a microsecond. Thus, the thermal effects on the etalon can be excluded over the millisecond time scale of the firing of the weapon if the transducer head is designed to ensure minimal conductive or radiative heat flow into the etalon and an accurate pressure transient response can be recorded. The practical considerations of this are discussed when the transducer assembly is described.

The values previously derived for the pressure and temperature sensitivity of the etalon are approximate due to uncertainties in the physical properties of the sapphire, extrapolation to a wider range of conditions, and the anisotropy of the material.

3.3 Etalon Design. An etalon is characterized by its free spectral range, which is the spacing between adjacent maxima (or minima) of the interference pattern. The free spectral range is determined by the thickness of the etalon and the refractive index of the material; the etalon used here has

$$FSR = \frac{c}{2nz} = \frac{3 \times 10^8}{2 \times 1.75 \times 0.005} = 17\ GHz. \qquad (13)$$

Generally, etalons have reflective coatings applied to the two parallel surfaces; this increased reflectivity results in the etalon having a higher finesse (Born and Wolf 1975) (i.e., the interference minima are narrower) than if no reflective coatings were used, and the peak reflected intensity is increased relative to the incident intensity. The finesse of an etalon is defined to be the ratio of the free spectral range to the cavity bandwidth (i.e., the width of the interference maxima) and is given by the following:

$$F = \frac{\pi\sqrt{R}}{1-R},$$

where

$$R = \sqrt{R_1 R_2} \ . \tag{14}$$

To select the best coatings for the etalon for this application, we studied the effects of the reflectivity values of the etalon surfaces on the system performance. A property that can be derived for an etalon is the "contrast" of the interference pattern (viz., the difference in intensity between the maxima and minima). A detailed analysis showed that to achieve the maximum etalon contrast for a given average reflectivity ($R = \sqrt{R_1 R_2}$), the two surfaces should have equal reflectivities ($R_1 = R_2$). In this case, the contrast of the etalon is

$$C_e = \frac{4R}{1 + 2R + R^2} \ . \tag{15}$$

In choosing the etalon reflectivity value, there are two conflicting effects to be considered. A fairly high reflectivity is necessary to obtain a sufficiently large reflected signal level, but a fairly low reflectivity is necessary to obtain a low finesse etalon that has broad minima that can be clearly detected. A low finesse is especially important in this system, since the fringe shifts occur rapidly. The shape of the etalon interference pattern as a function of reflectivity is shown in Figure 3. The effect of the etalon reflectivity on different signal analysis methods was also investigated, with consideration for the presence of system noise. We concluded that $R_1 = R_2 = 0.50$ would provide the best compromise between signal level and signal shape and should yield good performance for this system. For $R_1 = R_2 = 0.5$, the average reflectivity $R = 0.5$, and $F = 4.44$, which is fairly low compared to most etalons but is appropriate for this application.

3.4 Detection Principle. Simply monitoring the shift of an etalon interference pattern as the pressure on the etalon changes does not yield sufficient information for unique measurement of a pressure transient. This is because if just a single interference pattern is detected, any observed fringe shift could be due either to a pressure increase or a pressure decrease; it is possible to detect that a change is occurring but not the direction of the change. However, for a sapphire etalon, its intrinsic birefringence allows the pressure and

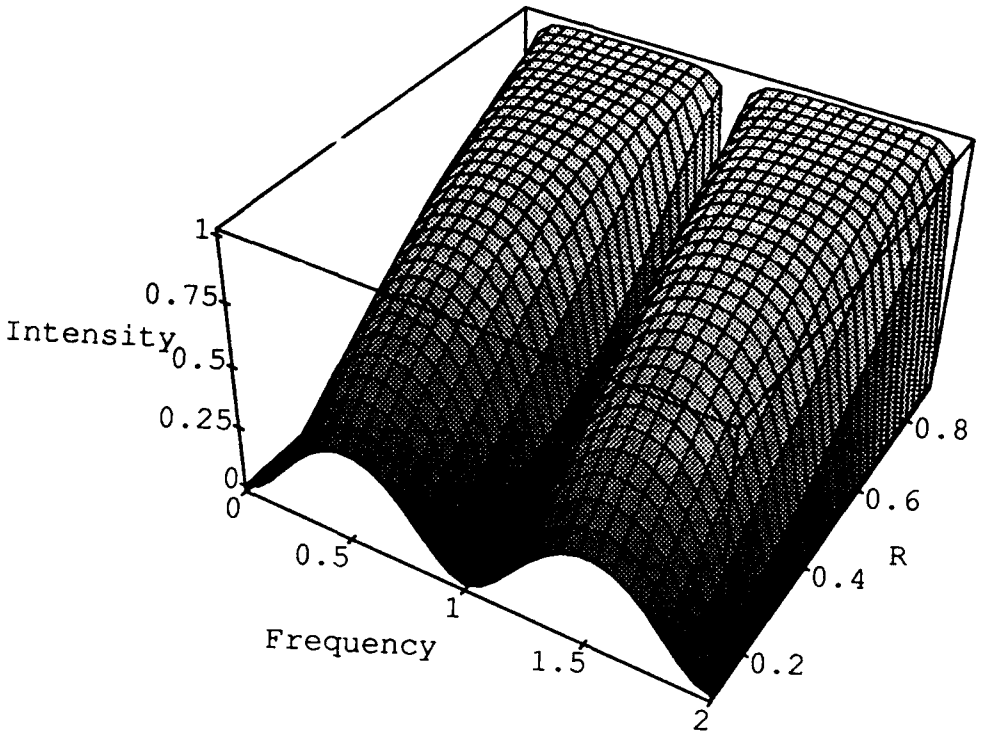

Figure 3. The Shape of Two Fringes of an Etalon Interference Pattern Plotted as a Function of the Average Reflectivity R of the Two Reflective Surfaces.

direction of pressure change to be determined uniquely. For an appropriately cut etalon, the interference patterns for the two orthogonal polarizations of the reflected signal are out of phase, as shown in Figure 4. Thus, by detecting the two polarization components of the signal from the etalon, both the magnitude and the direction of a pressure change can be determined. If the pressure is increasing, the signal for one polarization component will lead the signal for the other; but if the pressure is decreasing, the first signal will lag the other.

If a material which does not have this useful birefringent property was chosen for fabrication of the etalon sensor, another approach would have to be used. Alternative equivalent approaches would be to illuminate an etalon with two distinct wavelengths and monitor the two resulting interference patterns to obtain the two distinct signals or utilize a pair of etalons with different lengths, side by side, in order to obtain two out-of-phase signals. Both of these alternatives are more complicated to implement than the approach used here, which requires just a single source and a single etalon.

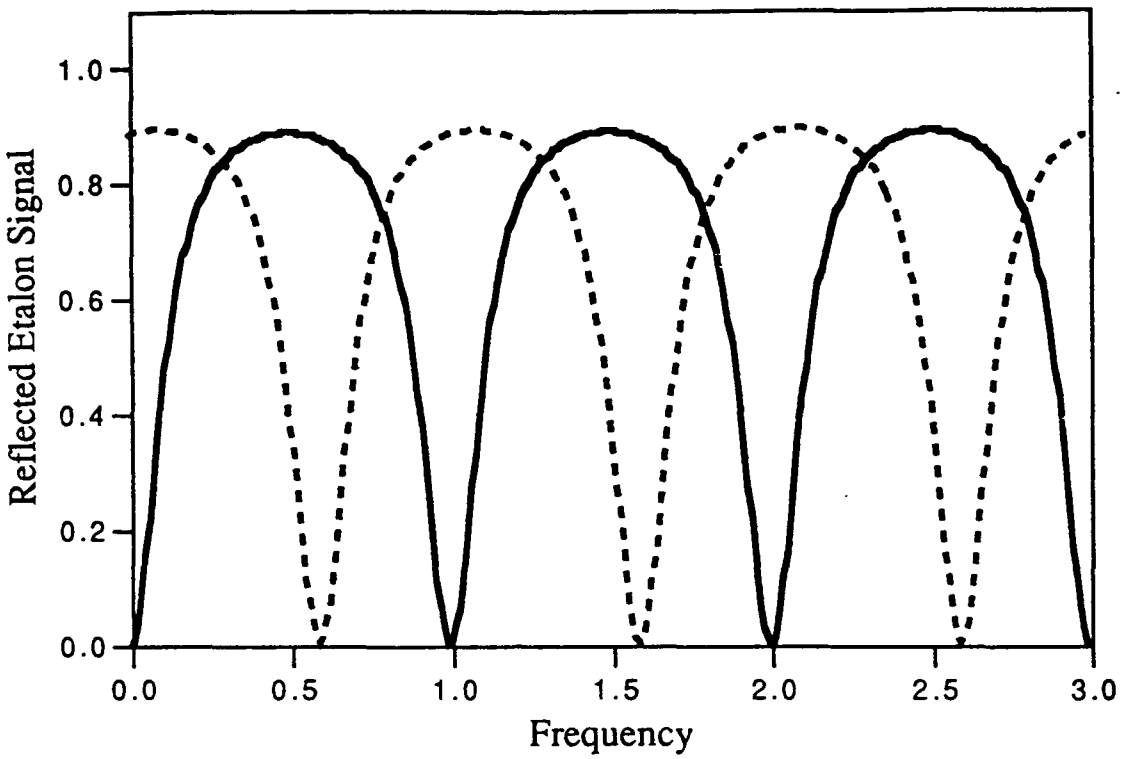

Figure 4. The Two Interference Patterns That Are Observed From a Birefringent Etalon When the Total Signal Is Analyzed Into Two Orthogonal Polarization Components That Correspond to the Two Axes of the Etalon.

By using a thicker transducer, it would be possible to increase its sensitivity (since the etalon free spectral range would be decreased) and so attain higher measurement accuracy. However, it is probably not practicable to use transducer thicknesses much larger than 10 mm, so only a factor of 2 improvement may be gained by this means. We conclude from the above that sapphire is essentially ideal for use as a transducer material in this system.

4. SYSTEM COMPONENTS

A schematic layout of the various components comprising the system is shown in Figure 5. The individual components are discussed in detail.

4.1 The Laser Source. The recently developed Non-Planar Ring Oscillator (NPRO), otherwise known as a Monolithic Isolated Single-mode End-pumped Ring laser (MISER), is particularly suited for use as a light source for performing sensitive interferometric measurements of this kind that previously would have been uneconomical or impossible. This

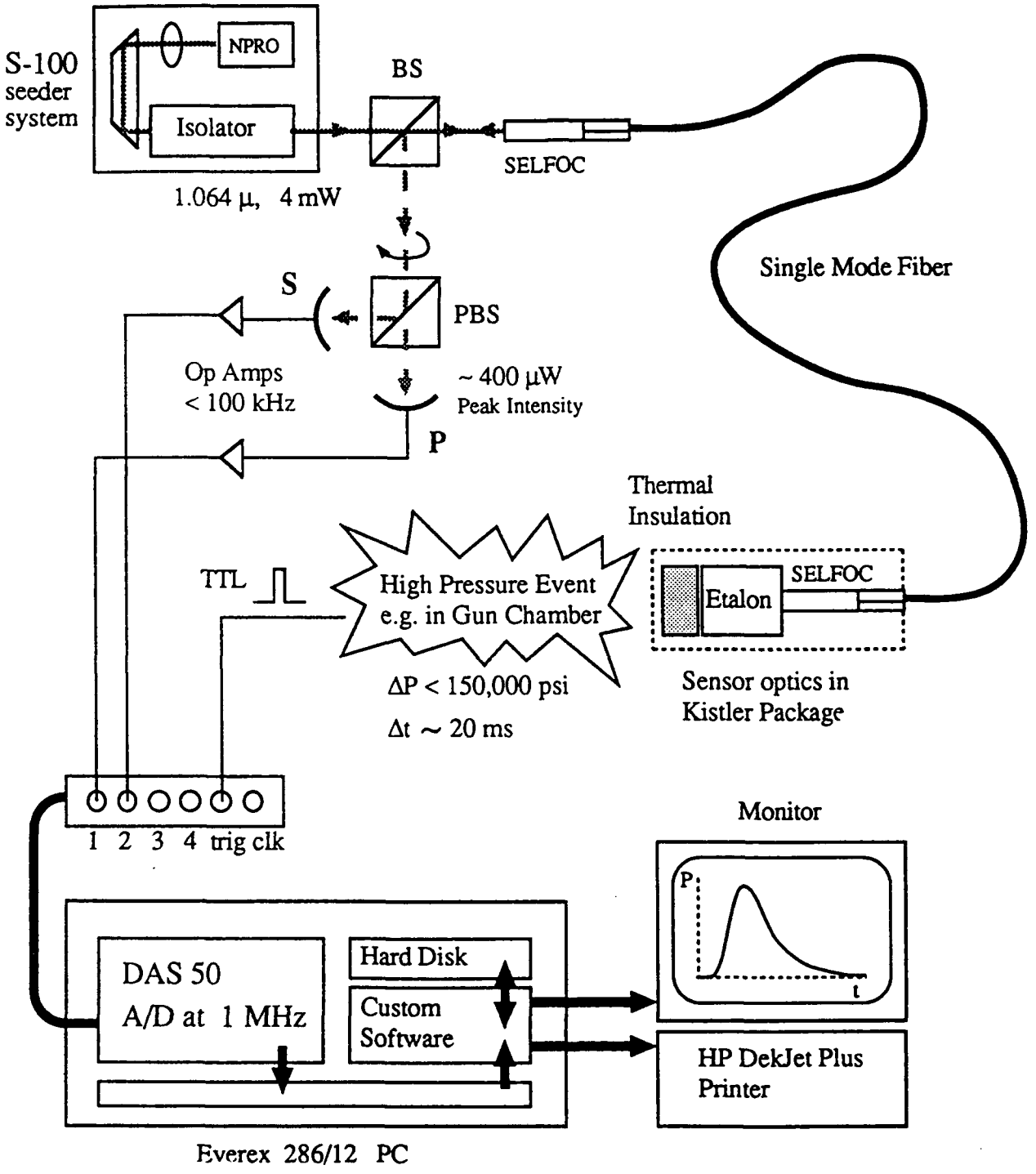

Figure 5. Schematic View of All the Components of the High Pressure Transient Measurement System.

single frequency diode-pumped solid-state laser (Kane and Byer 1985; Zhou et al. 1985; Schmitt and Rahn 1986) provides a cw output which has an ultranarrow linewidth and is frequency stable, independent of the output power, with good amplitude stability and immunity to feedback. LIGHTWAVE Electronics is currently manufacturing and selling NPROs to a wide variety of end-users, mostly for research applications. (This and other LIGHTWAVE products were partially or fully developed under the Small Business Innovative Research program.) NPROs having outputs at both of the Nd:YAG wavelengths of 1.06 and 1.32 μm are available. For this system, an NPRO source with wavelength 1.06 μm was chosen since the shorter wavelength offers higher sensitivity and also higher power than the 1.32 μm source. The frequency of this source may be tuned thermally over a moderate range (about 100 GHz) by changing the temperature of the laser crystal.

In order to obtain a low noise system that will provide the required accuracy, it is necessary to have a low noise optical source. The NPRO source has a linewidth of 5 kHz, many orders of magnitude smaller than the 17-GHz free spectral range of the etalon used, so that the frequency noise of the source is negligible in this application. The amplitude stability of the source is <1% rms at frequencies around the line frequency and the relaxation oscillation frequency in the region of 300 kHz. At other frequencies, the intensity noise is virtually zero (RIN < -100 dB/Hz). So the source contributes minimally to intensity noise in the system.

The NPROs generate a high quality diffraction-limited beam, which facilitates efficient coupling of their output into single mode fiber as required for this application. In this system, large back reflections are present, arising at a low level from the optics used to couple the beam into the optical fiber and more significantly from the reflected signal returned from the etalon. Both of these reflections are directed essentially back along the incident direction (i.e., right back into the laser crystal). Since large back reflections that enter the laser cavity can destabilize it, it is necessary to isolate the source from these reflections. Consequently, the laser source used for this system is a LIGHTWAVE Electronics S-100 laser; its main application is to seed much higher power YAG lasers, and consequently it includes an integrated optical isolator with a rejection ratio of 100,000:1, regardless of the polarization. This provides more than sufficient isolation for this application.

4.2 Fiber Coupling. Techniques for handling single mode optical fiber and for coupling of the laser output into single mode fiber to convey the light to the etalon were thoroughly investigated. Since the LIGHTWAVE NPRO lasers have a high quality TEM_{00} beam, their output can be efficiently coupled into single mode fiber. Coupling of the output beam of the S-100 laser source into single mode optical fiber is, in principle, simple and straightforward; it requires that the laser beam be focussed down to a waist size comparable to the size of the mode that propagates in the fiber. However, a single mode fiber for operation at $\lambda = 1.06$ μm has a mode diameter of just 7.7 μm and an NA of only 0.11, so that careful alignment of a tightly focussed spot is required in order to obtain a good coupling efficiency, and a mechanically stable coupling arrangement is required in order to maintain the coupling for extended periods and to prevent vibrations from altering the level of the coupled power.

For initial experimental tests in the laboratory, a Newport single mode coupler together with a microscope objective was used. This yielded a coupling efficiency of up to 45%. However, this approach uses a bare fiber end mounted freely in air, and the microscope objective does not have AR coatings on the lenses appropriate for the laser wavelength. Consequently, alternative methods of performing the coupling that have higher efficiency and would be more robust for use in the prototype device were investigated. A more appropriate method for obtaining the fiber coupling is to use a gradient index (GRIN) rod lens, otherwise known by the trade name of SELFOC™ lens, manufactured by Nippon Sheet Glass (Japan). These are glass rod lenses which have an index of refraction which decreases as the square of the radial distance from the central optical axis. They have the same focussing properties as standard lenses with spherical surfaces; however, their rod form allows fibers or other flat optics to be directly connected to their ends. They can be cut and polished to a particular length so that any desired focal length value can be obtained. SELFOC lenses are available in 4 different types, each having a different numerical aperture (NA = 0.16, 0.37, 0.46, 0.60). The lenses are available in diameters of 1, 1.8, 2.0, and 3.0 mm with approximate effective diameters of 0.65, 1.0, 1.3, and 1.8 mm, respectively.

These lenses are extremely useful for coupling light into optical fiber, since by mounting the input fiber end directly to the output face of the lens, the incoming beam is focussed onto the fiber core and highly efficient coupling can be achieved. By using a layer of index-matching gel or UV-cure optical epoxy at the interface between the lens and the fiber

end, reflections from the lens output surface and the fiber input surface are virtually eliminated. A compact laser source to optical fiber coupler that employs SELFOC lenses is manufactured by OZ Optics. It utilizes a simple mechanical mechanism having three circularly arranged adjustment screws to obtain the angular and translational alignment of the SELFOC lens with respect to the laser beam. One of these coupling devices and a SELFOC lens appropriate for the laser wavelength and beam parameters was obtained from OZ. Using this device, a coupling efficiency of 65% was obtained. However, it had a relatively small adjustment range and proved fairly difficult to align the fiber using it, and so we believe that it would not perform adequately for use in this prototype system.

Instead, we decided to hold the SELFOC and fiber end in a mirror mount (allowing angular adjustments to be made) that was mounted on a small X-Y-Z alignment stage (allowing lateral and axial translational adjustments to be made). The X-Y-Z stage has adjustment screws with fine machine threads, allowing for finer adjustment than is possible with standard micrometer screws. This coupling arrangement is bulkier than the OZ coupler, but is easy to use and affords a wide adjustment range. The components selected perform quite adequately for this purpose, although the adjustment capability of the mirror mount is not quite as sensitive as might be desired. We selected the N2.0 style SELFOC for use as the coupling lens, since it has the lowest NA and yields the best coupling efficiency for the fiber we used (NA = 0.11). The input surface of the lens was coated with a high quality AR coating for $\lambda = 1.06$ μm to minimize the return signal from this surface and to reduce extraneous fiber etalon effects. Using this lens and the holder described above, the coupling efficiency ranged between 60% and 80%. The efficiency could have been further improved, close to 100%, by using additional lenses to transform the laser output beam size so that the spot size at the output end of the SELFOC exactly matched the diameter of the mode in the single mode fiber. However, that would have required additional components and added to the alignment complexity. Since the coupling efficiency obtained with one SELFOC yielded ample coupled power for this system, just one lens was used for the sake of simplicity.

4.3 Optical Fiber. The laser output beam and the return signal are conveyed using single mode optical fiber as indicated in Figure 5. Once the light is within the fiber, it is extremely easy to convey it close to the location of the sensor. Due to the high quality of currently available single mode fiber (attenuation levels around 1 dB/km are typically obtainable for near

infrared wavelengths), the use of the optical fiber link allows the laser source and electronic detection system to be placed at a large distance from the etalon without resulting in any significant decrease in signal level. This system requires single mode fiber that is specially manufactured for operation at the source wavelength (λ = 1.06 μm). This is a nonstandard fiber optic wavelength; fiber optic systems either operate at around 0.85 μm, utilizing inexpensive sources and silicon photodiodes for short distance and low data rate applications (e.g., LANs), or they operate at 1.3 or 1.5 μm, where there are attenuation and dispersion minima (respectively) for silica fibers, long haul, and high data rate applications. Consequently, single mode fiber for λ = 1.06 μm is a specialty fiber that is harder to obtain (standard telecommunications fiber that is single mode for λ = 1.3 μm supports more than one mode at λ = 1.06 μm). We used single mode fiber optimized for this laser wavelength, type F1060C manufactured by Lightwave Technologies (Van Nuys, CA), which has an attenuation of 0.9 dB/km. The attenuation of this fiber may thus be ignored due to the fairly short lengths of fiber used in this system (3–5 m between source and transducer). This fiber has the standard 250-μm methacrylate jacket and 125-μm silica cladding enclosing the 6.7-μm-diameter core. The mode field diameter is 7.7 μm and the NA is 0.11.

In order to get efficient coupling of the beam into and out of the fiber, it is essential that it have good quality end surfaces. This was achieved by treating each fiber end as follows. It was first stripped of its methacrylate jacket, then cleaved to obtain a mirror-like flat end surface. Next, the fiber end was mounted in a glass microcapillary tube (Nippon Electric Glass Co., Japan) with a diameter which closely matched the fiber diameter. Then, it was glued in place with UV-cure epoxy so that the fiber end surface was flush with the end of the capillary tube and cleaned and checked with a microscope before being used. The fiber end was then mounted right up against the end face of the SELFOC lens, and UV-cure epoxy (Norland 61) was used to obtain an index-matched connection and hold the end securely in place.

4.3.1 Connectorization. Use of the high pressure sensor system in the field would be made easier if there was a connectorized joint present on the fiber path between the laser and the sensor. This would allow different sensors to be installed easily while maintaining fiber coupling of the laser source. Consequently, we studied the use of single mode fiber connectors in this system. FC/PC-style connectors were selected as they are reputed to have

the lowest back reflection from the connection. These connectors were found to yield good coupling levels (80–90%). However, during initial testing, index-matching gel had to be carefully applied to the connection in order to eliminate the reflection at the connector interface which would otherwise lead to a substantial fiber etalon effect producing a number of additional etalons in the system.

During the first round of testing at BRL (discussed in Section 5.1), most of the test transducers used were connectorized, but we experienced problems with substantial reflections arising from the connector interface that could not be reduced with application of index-matching gel. Additional time was not available to solve this problem. Consequently, it was decided not to use connectorized transducers in this prototype system. As an alternative, each of the final transducers was assembled with a fiber coupling lens attached to its input end. It was found that once the mechanical fiber coupler has been correctly aligned, even if the coupling lens is removed from the coupler and then later replaced (in the same orientation as before in the mechanical coupler), the fiber coupling level is regained at close to its original value, and minimal adjustment is required to maximize it. Thus, the lack of a connectorized fiber does not increase the complexity of using the system particularly. However, the absence of the interface that would have been present between the connectorized ends substantially decreases the level of fiber etalon effects in the system.

4.3.2 Cabling. Since the single mode fiber we used was nonstandard fiber, it was not available from any supplier already contained within a protective cabling to provide for ease of handling and resistance to damage. Since unprotected optical fiber is easily damaged, we investigated methods for protecting it for use in the field. We obtained and tested various types of breakout tubing (empty cabling) through which the fiber can be threaded for protection. We selected the most flexible of these cabling types since it is easiest to work with; the other types placed undue strain on the fiber due to their stiffness. This breakout cabling has a 0.5-mm-diameter inner Teflon tube surrounded by many thin Kevlar strands that act as a strength member for the cabling, which is in turn surrounded by an outer 3-mm-diameter plastic coating. The Kevlar strands and outer coating were bonded to the end of the metal tube in which the SELFOC was mounted at the input end, and similarly to a metal tube bonded into the rear of the transducer housing (see Figure 6) in order to strain relieve the cabling properly.

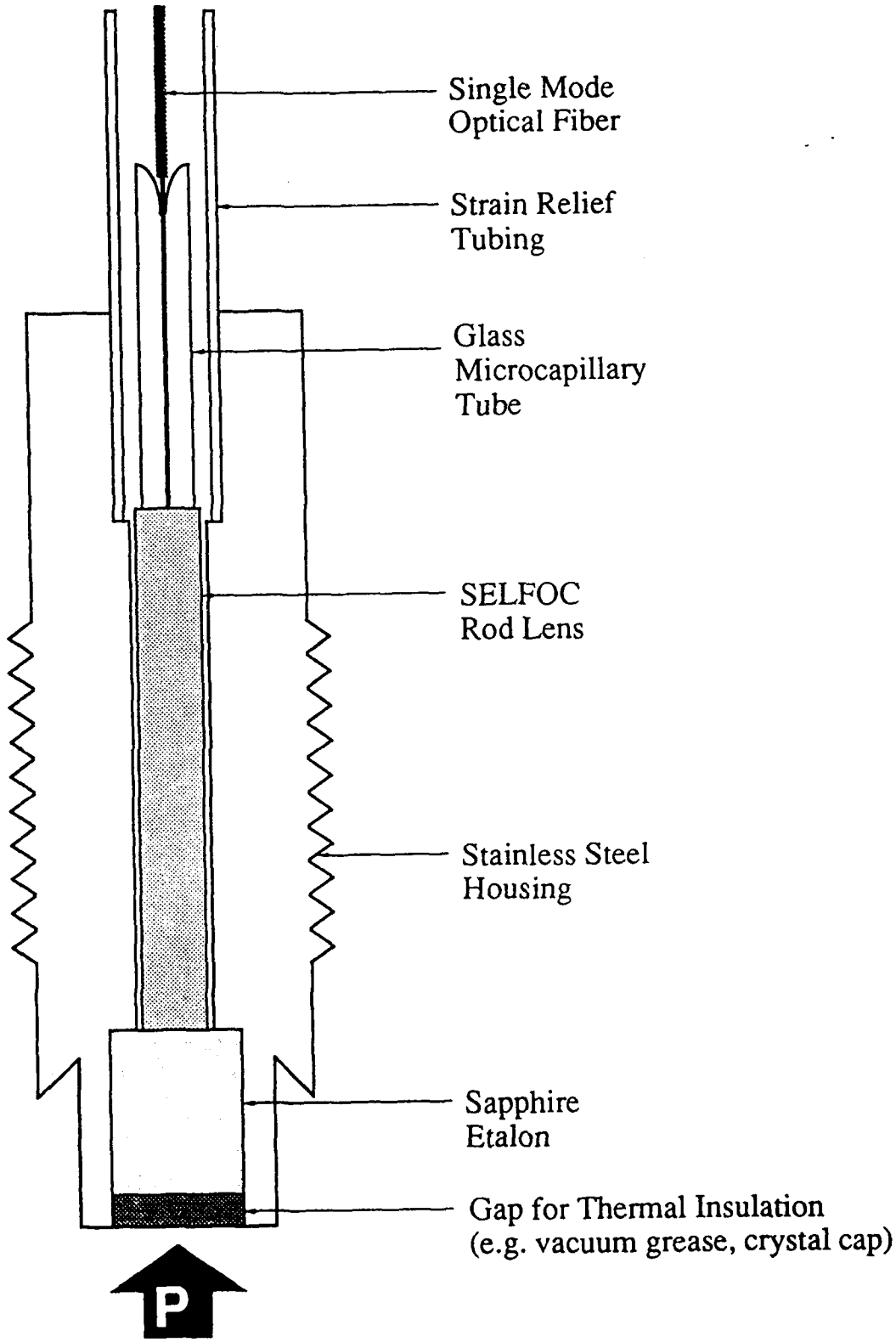

Figure 6. Schematic Design of the Transducer Head With the Optical Components Mounted in a Kistler 6211 Style Package. The SELFOC Lens Shown Is the N2.0, Which Was 16.35 mm Long. The S2.0 SELFOC, Which Is 6.54 mm Long, Was Also Used.

4.4 The Transducer Head. A major task of this research effort was the design and testing of the optical components of the transducer head. It was designed so that all the required optical components could be mounted in a Kistler 6211-style stainless steel transducer housing in order to maintain compatibility with the piezoelectric sensors currently in use at APG.

4.4.1 Etalon Fabrication. The sapphire material used for fabrication of the etalons was obtained from Crystal Systems, MA. It was supplied as 5-mm-thick disks, 25 mm in diameter, which were cut so that the normal to the flat surfaces made an angle of 6° with respect to the c-axis. The surfaces were then polished to be highly parallel (to within 5 arc-sec) with a surface quality of 60-40. The raw sapphire etalon material was tested using the S-100 as a light source, and it was verified that it had the desired birefringent properties; two interference patterns well out of phase were observed for the two orthogonal polarization components of the reflected signal. The 25-mm-diameter disks were cut into sections which were ground to yield 4-mm-diameter raw transducer etalons. They were chosen to be 4 mm in diameter since a larger size would not fit comfortably within the Kistler 6211 style housing. One end of each etalon had a bevelled edge ground on it so that it would seat well in the transducer head. The end surfaces were then coated by Virgo Optics, FL, to obtain partially reflective surfaces. Because of the harsh environment that they are to be subjected to, hard coatings were used as they are the most durable. The same coating was applied to each surface to obtain equal reflectivities of $R_1 = R_2 = 0.50$ (as motivated in Section 3). The coating was selected to have the desired reflectivity value when the external medium has n = 1.5 because UV-cure epoxy was used to bond the input surface of the etalon to a SELFOC and thermally insulating grease was used on the other end. As described earlier, the reflectivities of the two surfaces were selected to be equal, with $R_1 = R_2 = 0.50$. The spectraphotometer traces for the coatings indicated that they have the correct reflectivity values.

4.4.2 Transducer Design. The beam emerging from the transducer end of the fiber diverges in a cone determined by the NA of the fiber. A SELFOC lens is thus required at this end too, in order to obtain a collimated beam appropriate for probing the etalon. This is essentially the inverse of the process of coupling the laser beam into the fiber. This collimating lens also serves to couple the reflected signal from the etalon back into the single

mode fiber. Initially, the same type of SELFOC lens (N2.0, 16.35 mm long) that was used to couple the light into the fiber was used in the transducer head since it produces the best collimated output beam when attached to the output end of the fiber. Consequently, it should yield the best efficiency for coupling the reflected signal from the etalon back into the fiber. This lens type is available only as a 2-mm-diameter lens. Later, a different style SELFOC lens (S2.0, 6.54 mm long) was tested as an alternative for use in collimating the beam in the sensor head. Although this lens style does not yield quite as good a coupling efficiency as the one initially used in the transducer, it has less angular alignment sensitivity, and so should result in a transducer that is less susceptible to picking up vibrational noise and should make it easier to align the components during transducer fabrication. In practice, during assembly of the transducers, (some incorporated the N-type and others the S-type lens), it was found that there was a fair amount of variation of the maximum reflected signal level from the transducers which could not be correlated to the lens type used. Also, the assembly of the transducers incorporating the S-type SELFOC lens did seem slightly easier, but the task was largely limited by the alignment stage used.

It is easiest to illuminate the etalon transducer by making a direct optical connection between the etalon and the SELFOC lens. Consequently, the transducer material (4-mm diameter), SELFOC lens (2-mm diameter) and the end of the fiber, held in a microcapillary (1.8-mm diameter) were mounted in a Kistler 6211-style package as shown in Figure 6. It was possible to accommodate the 2-mm-diameter lens mounted directly behind the front surface of the etalon, since this arrangement still leaves sufficient material in the transducer body to support the etalon adequately without cracking or loss of pressure seal. A microcapillary tube serves to hold the end of the fiber in position adjacent to the lens inside the transducer. The schematic design of the transducer head was reviewed by Dr. Richard Beyer and others at BRL; they agreed that the design was sensible.

4.4.3 Pressure Seal. One of the issues we were initially particularly concerned about was obtaining a tight seal that could contain the high pressures that the transducer is exposed to. However, this proved easier than anticipated. On the advice of Dr. Richard Beyer of BRL, the pressure seal was accomplished in the same manner that he has previously used—simply by using a very thin layer of UV-cure optical epoxy (Lightweld) between the flat surface of the back side of the etalon and the surface of the stainless steel transducer body. To ensure that

a good bond was obtained that would provide the required pressure seal, the flat etalon surface was carefully cleaned and examined microscopically, and the transducer body was very well cleaned, including a final cleaning in an ultrasonic cleaner. The flat surface inside the transducer body on which the etalon rests was also machined to be as flat as possible. The optically flat etalon surface and the fact that such a surface can be cleaned very well no doubt facilitated obtaining a good pressure seal. We tested such seals using the Kistler hydrostatic high pressure generator and found that they held static pressures of up to 100,000 psi (the maximum pressure that can be generated by the hydrostatic generator used) repeatedly for periods of hours. Presumably, compression of the epoxy layer by the applied pressure maintains the seal.

4.4.4 Transducer Assembly. As anticipated, the assembly of the fiber coupled etalon transducers was time consuming and delicate work; the small size of the single mode fiber and its delicate nature means that it has to be handled carefully. A key aspect of the transducer head assembly process is the relative alignment of the fiber end, the SELFOC lens, and the etalon in order to obtain a high efficiency for coupling the reflected etalon signal back into the fiber. This was a nontrivial task requiring a good deal of careful investigation to obtain sufficiently good coupling between the fiber and the sensor. This procedure is complicated by the fact that the alignment is with respect to a "virtual source," and also the frequency of the source may be close to an interference minimum of the etalon given its length at the ambient temperature. Thus, the laser frequency has to be adjusted too, in addition to the component position, during transducer assembly. As a result, this alignment is similar to, but decidedly more difficult than, aligning the fiber input end with respect to the beam from the laser.

Different methods for performing this alignment were investigated. The initial approach that was used for assembling test transducers was the most straightforward. It involved simply using UV-cure epoxy to hold the etalon and SELFOC lens directly in place in a Kistler 6211-style stainless steel body that was precisely machined to accept the components. The fiber end was mounted in a microcapillary tube, inserted from the back of the transducer body, and adjusted with respect to the end of the SELFOC lens to achieve the best return signal before being cemented in place using UV-cure epoxy. Although this method does work, it proved difficult to implement, and low coupling efficiency was obtained so that the return signal level was fairly low.

An alternative approach was developed that yielded excellent signal levels; this entailed gluing the components together in a stepwise procedure and then cementing them into the transducer body. First, the etalon and SELFOC lens were bonded together with UV-cure optical epoxy (Lightweld) in a special gluing holder. Second, the fiber was aligned with respect to the input end of the SELFOC of this SELFOC-etalon assembly; this was the more difficult, tedious step. It required a special alignment stage with lateral and angular adjustment capabilities and a vacuum chuck for holding the end of the fiber. When the maximum reflected signal was obtained, the fiber end was bonded in place using UV-cure epoxy (Norland-61). Finally, the full assembly was cemented in place in the transducer body using a thin layer of UV-cure epoxy (Lightweld) between the back surface and sides of the etalon and the stainless steel body. Implementing this procedure required a sensitive alignment jig with a vacuum cnuck to hold the fiber end; one was borrowed from another project, and it accomplishes the task, but with difficulty since it was not optimized for this purpose. A more sensitive jig specially designed for this task would need to be assembled to make this task easier. Even though the alignment is difficult to achieve once it had been accomplished, a good return signal from the etalon was obtained. These transducers yielded peak return signals of 300–400 μW (for a laser source power of 4 mW). This exceeds the original estimates, which predicted a peak signal of 100 μW at best and of 10 μW at worst, depending on assumptions about the efficiencies in the system. We assembled a number of test transducers and four transducers for initial testing at BRL and five transducers for final delivery, according to this design. One of the final transducer heads is shown in Figure 7.

4.4.5 Thermal Sensitivity. As discussed in Section 3, the transducer material will also be susceptible to thermal effects, and any marked change in its temperature will lead to thermal expansion, increasing the etalon length that will distort the pressure measurement. Although there is a large temperature rise inside the gun bore during firing of the weapon, the overall temperature rise of the barrel is much smaller due to its large thermal mass. But a thermally insulating layer is required to protect the transducer material from the immediate effects of the temperature changes accompanying the pressure impulse. For the prototype transducers, the approach chosen is simply to cover the outer, exposed surface of the etalon transducer with a thermally insulating ablative layer, such as a layer of vacuum grease, as is currently used with the Kistler piezoelectric sensors. A more sophisticated approach that could be used in the

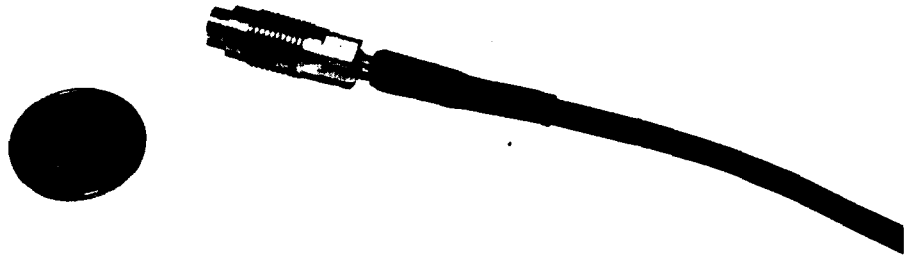

Figure 7. Photograph of One of the Final Transducer Heads That Was Supplied for Testing. A 25-Cent Coin Is Included to Set the Scale of the Device.

future would be to use a 1- to 2-mm-thick layer of a durable material such as cubic zirconia to obtain this insulation. While the pressure pulse will be transmitted essentially immediately through this layer, it will require hundreds of milliseconds for the temperature rise to propagate through it. The thermal conductivity of cubic zirconia (0.02 W/cm °C) is lower than most other optical crystals (providing the easiest way to distinguish it from diamond), so it is a good choice for a durable insulator.

4.5 Signal Detection. The reflected signal from the etalon collected by the remote end of the fiber in the transducer head is relayed back to the detection system located next to the laser source. The light exiting the fiber is collimated by the SELFOC lens used to couple the light into the fiber, and it then passes through the nonpolarizing beam-splitter cube (T = 51.6% for P-polarization and 49.3% for S-polarization at λ = 1.064 μm with negligible loss) where half of the signal is deflected out towards the detectors, while the other half is lost, heading back along the direction of the laser beam. The deflected half of the signal passes through a polarizing beam-splitter cube (T = 99.4% for P-polarization, and R = 99.8% for S-polarization at λ = 1.064 μm) which acts as an analyzer, separating the two orthogonal polarization

components of the interference signal; the P-polarization component passes straight through to reach a photodiode, while the S-polarization component is deflected towards a second photodiode. The photodiodes serve to convert the optical signals to electronic signals for recording and display purposes. Given that the signal level is in the range of 10–400 μW, no highly sophisticated photodetector is needed, although a fairly fast response and wide bandwidth are necessary to detect the rapidly varying interference signals. We selected EG&G YAG-200 silicon PIN photodiodes since they have enhanced sensitivity in the near infrared range (including $\lambda = 1.06$ μm) compared to other silicon photodiodes, and they have a 5 ns rise time, faster than required for this application. Simple compact transimpedance amplifiers were used to amplify the photodiode signals to obtain output levels appropriate for input to the A/D converter board. The laser power supply was modified so that it could power these amplifiers too, making an additional power supply unnecessary.

Direct monitoring of large caliber chamber pressure waveforms normally requires a detection system response of 5–10 kHz (Walton 1983). But due to the rapidly varying nature of the interference pattern signal in this system, a wider bandwidth response is required here. The pressure transients typically have rise times of the order of milliseconds (for instance, see Figure 11). Dr. Richard Beyer indicated that this prototype sensor system should be able to measure a maximum pressure change of not more than 3,000 psi over a period of 10–20 μs. Since the 5-mm-thick sapphire etalon produces a fringe shift for every 4,300 psi of pressure change, the maximum rate at which the interference fringes will shift will be equivalent to about a 100 kHz signal. Because the optical signal level was larger than anticipated, the photodiode amplifiers could operate with reduced gain, which improved their frequency response. Figure 8 shows the variation of the output of the photodiode-amplifier combination as a function of the frequency of the optical input to the photodiode. The response is essentially flat out to 200 kHz, after which it rolls off slowly. This is double the 100-kHz bandwidth required to monitor the fastest signals expected in the sensor system. The sensitivity of these photodetectors at $\lambda = 1.06\mu$ was set so that for a typical peak signal from the etalon, they produce an output of about 3–6 V, suitable for input into the A/D converter board, which can be set to the unipolar ranges of 0–5 V or 0–10 V.

4.5.1 Optical Power Budget. The higher the signal level received from the etalon, the better the performance of the system. Given that the source has a fixed output power

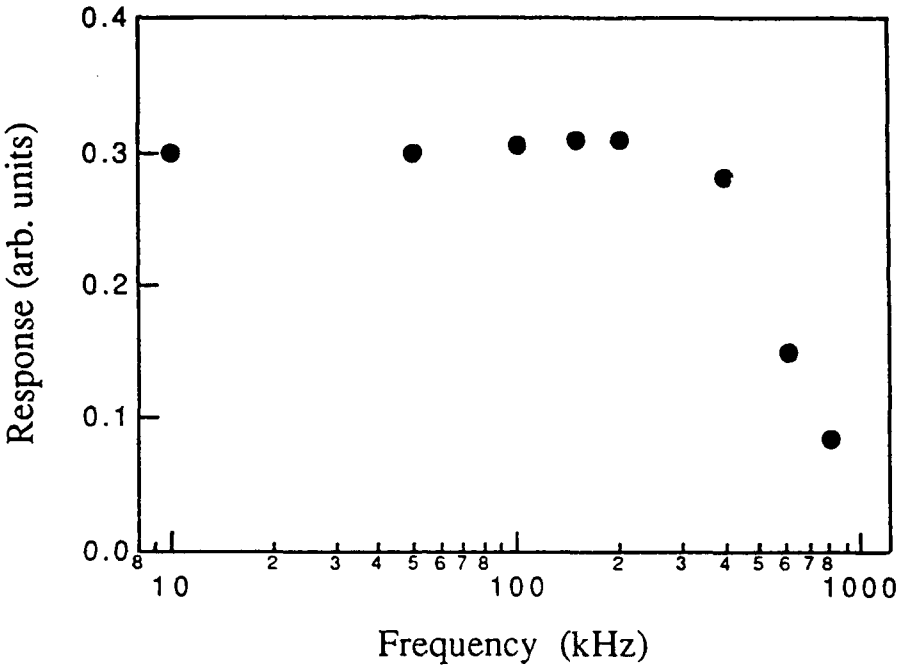

Figure 8. Response of the PIN Photodiode and Transimpedance Amplifier Combination as a Function of Frequency.

(4 mW), the signal level depends on the coupling efficiency of the system. Unfortunately, some large losses are inherent in this system. The major loss arises from the 50-50 beam splitter required to pick off the returned signal reflected from the etalon. It first reduces the level of optical power that can be coupled into the fiber by 50%. Secondly, it deflects only 50% of the returned etalon signal towards the detectors. The fiber coupling efficiency with the chosen focussing arrangement was 80% at best and more typically was 70–75%. The peak reflected signal from the etalon is less than the incident power level, since the etalon has a fairly low finesse. In this case, the peak signal is 89% of the incident power. These well-defined losses together limit the system efficiency to be no greater than 17.8%. Losses arising from the AR-coated surfaces of the beam splitters and the coupling lens are quite low, and the loss from signal attenuation in the fiber is negligibly small. The main additional losses that are present are due to inefficient coupling of the signal into and out of the transducer optics. The observed peak signal received at the detectors was around 400 μW, which corresponds to a 10% total system efficiency. Thus, the excess loss due to all other sources, over and above the well-defined losses quantified previously (17.8%), is around 56%. This is fairly good and substantially better than was initially expected.

It is important that there are no additional reflections present in the system that could result in a significant background light level reaching the detectors that would mask the desired signal from the etalon. Most of these reflections were anticipated during the design of the system and were minimized by the use of AR coatings on exposed surfaces and by index matching at interfaces between components so as to minimize the reflectivity of the interface. However, it was found that there was a substantial background signal resulting from the half of the laser beam that is split off initially by the beam splitter because a small fraction of this was being reflected back to the detectors by the side of the box enclosing the laser, fiber coupler, and detectors. This background source was easily eliminated by the use of an absorbing material in this beam path to prevent this reflection.

After all additional reflections have been reduced as far as possible, there still remains a low background level that reaches the photodetectors that is due to residual reflections from the AR-coated surfaces of the beam-splitting cube and the fiber coupling lens and the other interfaces in the system. This background level was observed to be around 15–35 μW, which is a small fraction of the peak signal of around 400 μW.

4.5.2 Noise Sources. Since this system measures the interference pattern directly (as opposed to a phase measurement scheme), it will be susceptible to changes in the optical signal level that arise from any noise sources (i.e., outside influences other than that being measured [e.g., thermal drifts]). However, since the high pressure measurement system is designed to measure only brief impulse events on a time scale of milliseconds, it will not be affected by the long-term intensity fluctuations that cause problems in more typical systems that measure physical values over longer periods such as hours or days. However, additional short-term fluctuations can arise from the source, detectors, variations in the coupling efficiency between elements of the system, or additional interference effects. In this system, source fluctuations are at a very low level and do not influence the measurement. Similarly, the photo detectors contribute no noise in excess of shot noise, which is well below other noise sources in the system.

Intensity noise can arise from variations in the coupling between different elements (for instance, the coupling of the beam into the fiber, coupling of the beam into and out of the transducer, and coupling of the signal back to the detectors). In particular, vibrational noise in

the surroundings can result in changes in the coupling efficiencies. A major contributor to system noise when the first few transducers were built was the vibrational sensitivity of the transducer coupling due to the method used to strain relieve the fiber cabling. This and other possible sources of noise arising from changes in coupling levels have been eliminated by careful, stable mechanical mounting of the optical components and by appropriate strain relief of the cabling, which makes the transducer optics much less susceptible to vibrations. It is also possible for intensity variations to arise due to increases in attenuation if the optical fiber is bent unduly, although this only occurs when the fiber is bent through small radii of the order of a few centimeters. This is easily avoided by ensuring that the fiber is not bent through any tight radius at any point.

Another source of noise is stray interference effects. Because of the interferometric approach used, additional reflecting interfaces in the system can lead to extraneous, undesirable etalon effects that result in a noisy output signal. The most significant effect arises when the fiber is between the two reflective surfaces that cause the interference, since the fiber is long and flexible, so that thermal drifts and vibrations lead to fluctuations in its length. As there are two fairly high reflectivity surfaces on the etalon ($R_1 = R_2 = 0.5$), any other interface with nonnegligible reflectivity at the input end of the fiber can result in the presence of an extended etalon which incorporates the fiber. Consequently, the critical interfaces are the front surface of the input SELFOC and the interface between the SELFOC and the fiber. Even a low reflectivity at the input end of the fiber combines with the $R = 0.5$ interfaces on the etalon to form an additional fiber etalon which can result in significant amplitude variation of the detected signal. The contrast value for etalons having various reflectivity values at one surface (R_1) and a reflectivity of $R_2 = 0.5$ at the other surface are shown in the following table.

R_1	R_2	Contrast	Comment
0.5	0.5	0.889	Sapphire etalon
0.04	0.5	0.283	Uncoated silica surface in air
0.01	0.5	0.141	—
0.005	0.5	0.100	—
0.0025	0.5	0.071	—
0.001	0.5	0.045	AR-coating specification

It is seen that a silica surface (n = 1.45) that is uncoated (R = 0.04) will combine with the R = 0.5 surface of the sapphire etalon to generate etalon effects with a peak signal that is 28% of the incident signal level. This is clearly unacceptable, so that an AR coating is essential on the input surface of the SELFOC. Even the residual reflectivity of the AR coating (0.01) will contribute some noise at the 4–5% level. Clearly, the interface between the SELFOC and the fiber must also be well index matched; a residual reflectivity there of only 0.005 will still contribute etalon effects at the 10% level. The reflectivity of this interface was reduced to about 0.001 by carefully bonding the two surfaces with UV-cure epoxy.

Due to the length of the fiber, the fiber etalon effects have a small free spectral range. For instance, for a fiber length of 3 m, the free spectral range is

$$FSR = \frac{c}{2nz} = \frac{3 \times 10^8}{2 \times 1.45 \times 3} = 34\ MHz. \qquad (16)$$

Thus, the ratio of the FSR of the fiber to the FSR of the etalon is about 500. Consequently, the fiber etalon is about 500 times more sensitive to thermal effects than the sapphire etalon. The longer the fiber, the smaller the FSR, and the more sensitive it will be.

As mentioned above, background reflections were minimized by index matching at the interfaces, and by using an AR coating on the input SELFOC lens, so fiber etalon effects should be small. They should be observable at a low level if the etalon signal is monitored while the laser frequency is scanned; they appear as a low amplitude, rapidly varying interference signal superimposed on the main interference signal. Luckily, when the laser frequency is fixed, these effects are relatively slowly varying due to their thermal origin (time scale of fractions of a second), so they don't have much effect on the measurement of a rapid high pressure transient (time scale of milliseconds).

Because the system relies on the alignment of the laser polarization with respect to the etalon axes and the resolution of the reflected etalon signal into the two correct orthogonal polarization components, noise on the output signals can also arise from changes in the polarization state of the beam transmitted through the fiber. Perfect single mode fiber would maintain the state of polarization of a beam propagating through it. However, impurities and

nonuniformities in the fiber as well as outside influences, such as when the fiber is unduly bent or twisted, result in a disturbance of the polarization state. The degree to which the polarization is altered depends on the fiber length and the level of the disrupting influences. For short lengths (a few meters), the polarization will usually be preserved to a high degree provided that the fiber is not twisted or bent through a small radius (say less than 10 cm). Specially manufactured polarization preserving fiber is available, but it is designed to preserve only linear polarization along one fixed, preferential axis. It will also preserve linear polarization along the axis perpendicular to the preferred axis, but that axis is highly bend sensitive. Actually, the fiber is birefringent, with a slow and a fast axis. So although it can preserve the polarization of a beam with linear polarization parallel to one of the axes, it cannot preserve the general polarization state of the signal reflected from the birefringent etalon, since its orientation is time varying as the etalon length varies. Thus, this polarization signal would be scrambled if it was transmitted through polarization preserving fiber. What is required for this application is true polarization preserving fiber, which does not yet exist; only single component polarization preserving fiber is available. Consequently, plain single mode fiber must be used in this system, with every effort being made to ensure that the state of polarization is undisturbed. This requires that the fiber connection be of minimal length and that bending and twisting of the fiber during the measurement when the weapon is fired be reduced as far as possible. The degree to which the polarization of the signal can be maintained in the field may be the ultimate limiting factor for the performance of this system.

From the previous discussion, it is clear that there are a number of noise sources in this system which have to be dealt with carefully and which could probably never be totally eliminated. A realistic goal is to reduce residual intensity fluctuations to no more than a couple percents, which have been achieved in a laboratory environment.

4.5.3 Polarization Alignment Procedure. In order to make use of the two independent signals from the birefringent etalon to allow the direction of the pressure change to be monitored, it is necessary to obtain correct alignment of the laser polarization, and the analyzing beam-splitter cube with respect to the etalon axes before a measurement is performed. Since the orientation of the axes of the etalon are initially unknown, the alignment procedure requires some iteration to achieve optimum alignment. The orientation of the laser polarization can easily be altered by rotating the half-wave plate that is positioned at the

output port of the laser head (the angle of the polarization is rotated by twice the angle through which the half-wave plate is rotated). To allow for the signal reflected from the etalon to be resolved into the appropriate polarization components and for correct alignment of the photodetectors, the polarizing beam splitter (analyzer) and the two detectors were mounted in a compact rotatable assembly. This allowed for 360° of rotation of the beam splitter about the axis defined by the reflected signal beam, so that the beam could be resolved into any desired polarization components while maintaining the correct alignment of the two photodiodes with respect to the two component beams.

Two main steps are required to achieve the desired polarization alignment. First, one of the etalon axes must be located by varying the orientations of the half-wave plate and analyzing beam splitter until one signal received from the etalon (say the S signal) is at a minimum value and remains at that level even when the laser frequency is scanned. This corresponds to having the laser polarization aligned parallel to one of the etalon axes, so that only one etalon component is excited, and to having the analyzer axes parallel to the etalon axes. This is illustrated schematically in Figure 9a. The second step is easy; the half-wave plate is rotated by 22.5° (in either direction) so that the laser polarization is then oriented midway between the two etalon axes, so that both etalon components are equally excited (Figure 9b). The analyzer position does not need to be altered since it is already in the desired orientation. The alignment can be carefully checked by measuring the two etalon interference patterns using the program SCAN (see Section 4.7) while scanning the laser frequency. Further details of this procedure are given in Section 7.

4.6 Data Acquisition System. Once the two interference patterns from the etalon have been converted from optical to electrical signals, it is necessary to extract the pressure information from them. Since the gun chamber pressure transients that are to be measured with this system are short, fast events, the signals can be monitored using a transient digitizer or digital scope, and the data could be visually analyzed after the event or transferred to a PC for analysis. However, this requires expensive monitoring equipment and makes the data handling more cumbersome. Another approach would be to use custom hardware (i.e., electronic fringe counting circuitry) to monitor the fringes as a function of time. However, due to the nontrivial, multivalued nature of the relationship between the shifts in the interference

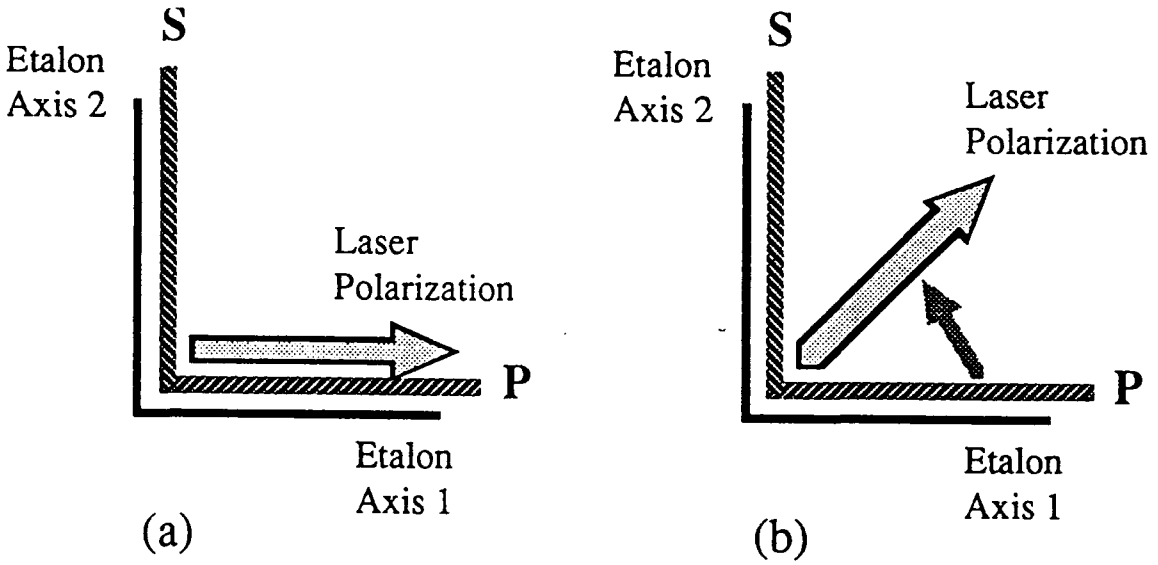

Figure 9. (a) The Laser Polarization Must First Be Aligned Parallel to One of the Etalon Axes, With the Analyzer Axes Parallel to the Etalon Axes Too. (b) Then, the Laser Polarization Must Be Rotated by 45° to Bring it Midway Between the Two Etalon Axes So That Both Are Equally Excited.

pattern and the pressure changes, it would be more difficult to extract the desired information using such dedicated hardware. Also, because the pressure change results in a shift of the interference pattern of a fairly small number of fringes, to obtain good pressure resolution would require resolving fractions of a fringe shift. But hardware circuits would be limited simply to counting fringes which would only permit a resolution comparable to one fringe to be obtained.

An alternative approach would be to digitize the interference signal directly using an analog-to-digital (A/D) converter and then use software implemented on a personal computer to determine the pressure values from the digitized data. This is a more involved approach but would provide more flexibility. It allows access to the raw interference pattern data so that the performance of the system can be studied more closely, and the data can be stored as files on disk, providing convenient long term storage, allowing for it to be recalled later as required, and permitting subsequent analysis and the direct numerical comparison and

manipulation of signals. Also, the resolution of the measurement system can then be improved greatly by using detailed signal analysis routines to resolve small fractions of a fringe shift.

Because of these advantages, we decided to base the data acquisition system on an A/D converter and a personal computer controller. The type of computer to be used was limited to IBM-style PCs since they are in widespread use at BRL. Since the high pressure events being studied at BRL are of short duration, the feasibility of this approach depends on the availability of an A/D converter board that can perform the digitization at a sufficiently high speed for capturing the details of the interference pattern shifts. As discussed above, the maximum signal bandwidth expected in this system is 100 kHz. According to the Nyquist Sampling Theory, the sampling rate must be at least twice the highest frequency in the signal to be digitized. In practice, the multiple is usually between 3 and 10 times the maximum frequency of interest. Since two fringes need to be monitored simultaneously, this measurement system requires an A/D conversion rate of around 1 MHz. This is much faster than most available A/D boards, but the DAS-50 manufactured by Metrabyte can run at this rate. This board is well matched to the requirements of this system, and so it was the one selected. It has an on-board memory of 256 kilobytes, which is expandable up to 1 Megabyte. It can be run at conversion rates from 137 Hz to 1 MHz and can be triggered in a variety of ways.

This A/D board can only operate with computers which utilize the PC-bus, such as the IBM AT-style PC or similar IBM-compatible PCs available from other companies. After studying reviews of the wide variety of these computers that are available, we selected an Everex STEP 286-12 system. The computer has operated without problems over the last ten months. To obtain hard copy of text and graphics, we purchased an HP DeskJet-Plus printer, which is inexpensive, yet produces good quality output (300 dpi resolution) and is very suitable for use with this system.

The DAS-50 A/D board is a plug-in card, so it installed directly into the PC cabinet. To test its performance, waveforms from a signal generator were digitized, and the data points were written to the hard disk for a variety of signal frequencies and conversion rates. Plots of the data points showed that the A/D board performs according to specifications and can

indeed operate at the maximum conversion rate of 1 MHz. The A/D board has worked well and seems appropriate for use in this system.

4.7 Data Acquisition Software. Custom software specifically for control of the collection and storage of digitized data acquired using the A/D board and for analysis and presentation of this data was developed for this system. A data acquisition program (named ACQUIRE) was written to set up the A/D board with suitable default parameters for acquiring data during a pressure transient measurement and for controlling the acquisition of this data. The program sets values for the number of samples to be acquired, the digitization rate, the analog signal input range, and the trigger mode type and level. If any of these values need to be modified, a pop-up screen can be displayed that has fields showing the default values for the various parameters which can then be modified as required. The program then waits for a trigger signal, which initiates acquisition of the data to the on-board memory. For the measurement of transient events, the data acquisition occurs at a high rate and is over in a fraction of a second. So the trigger signal must be generated immediately prior to the pressure transient to be measured in order to not fill the on-board memory (256 kilobytes) before all the required data is accumulated. After the measurement is performed, before the program completes execution, it allows for the first 32,000 data points to be copied from the memory of the A/D board to a file on the hard disk that can be read back for subsequent display and analysis. The file is written in a form suitable for immediate display by graphics routines. If the data set is particularly large or if only some particular subset of it is required, then a separate storage routine (named STORE) can be used to copy the data to the hard disk as required. All the data acquisition programs were written in FORTRAN and compiled using the Microsoft version 4 compiler.

In order to ease the programming task, the display and analysis of the data was based on a software package called "PC Data Master" that provides graphics, analysis, and hard copy routines suitable for the handling the digitized data. This package is not particularly sophisticated or complicated to use, but performs the necessary tasks. It provides a shell which implements independent DOS console and graphics screen windows and has flexible graphics routines and numerous data file math routines. It allows user-specific data processing steps to be incorporated as independent executable files written in any language. Using this package, graphs of the data can be drawn straightforwardly and printed directly on

the DeskJet printer. Also, its routines allow for easy manipulation of the data and display of the results. An alternative data analysis package that could be used instead is Snapshot Storage Scope. We did not purchase it since it is already available at BRL.

A complete, operational system requires custom software for rapid analysis of the etalon signals. We devised a specific signal analysis method that extracts the pressure change from the etalon signals as well as continuously monitoring the direction of the pressure change. The pressure change is determined by fitting the fringe pattern to the known functional form, given the etalon reflectivities. The direction of pressure change is determined by monitoring one of the interference signals (say the S signal) as a parametric function of the other (say the P signal). If the pressure is increasing, then this traces out closed loops with a particular direction of rotation (say clockwise), while if the pressure is decreasing, then this traces out closed loops with the opposite direction of rotation (say counterclockwise). (This is similar to the generation of Lissajous figures.) Specific routines for the analysis of the etalon signals have not been developed yet since we have not performed any transducer testing in gun chambers; so no realistic test data is available on which to base the analysis. In particular, the level and type of system noise has not yet been quantified. Custom analysis routines to interpret the digitized signals from the transducer await the next phase of development. This can also be undertaken by personnel at Aberdeen who have expertise in this and will be performing the testing.

A second data acquisition program (named SCAN) that was similar to ACQUIRE was written for performing low rate acquisition of a small sample of data to be used for scanning through the etalon interference pattern when aligning the laser polarization and analyzing beam splitter with respect to the etalon axes. It was used in conjunction with PC Data Master routines to perform a detailed study of the etalon response as a function of the polarization of the laser beam incident on the etalon for verifying the procedure for correct mutual alignment of the laser polarization and the analyzing beam splitter with respect to the etalon axes. This data, together with other data taken during evaluation of the transducers as well as signals from a signal generator, were used for testing the logging, storage, and retrieval of data with this data acquisition system. This allowed for checking and fine tuning of the programs to ensure that they performed as required.

4.8 System Integration. The mechanical, electrical, and optical components were fully integrated and tested and perform as required, yielding a compact, integrated prototype system that was delivered for use at BRL. The laser head, fiber coupler and detector optics, and electronics were mounted on a single rigid base plate to maintain their relative alignment. Sides were attached to the base plate, and a cover was placed on top of the sides to provide a solid aluminum box to protect these components. This enclosure is 15 1/2-in long, 11 1/2-in wide, and 6 1/4-in high. The enclosure was made fairly large to provide ample space within it to allow for easy adjustment of the optical components. The sides and top can each be separately removed to gain access to the various components. In addition to this box and the fiber-coupled transducer, the complete system consists of the separate laser power supply and the personal computer and printer as shown in Figure 10.

5. TESTING AND RESULTS

The complete development of a practical high-pressure transient measurement system requires extensive testing of the transducers—static and dynamic testing and calibration in the laboratory (using, e.g., a hydrodynamic generator), as well as field testing (i.e., in a gun chamber)—that would need to be coordinated with personnel at BRL. This variety of testing methods is necessary since laboratory testing is usually more accurate (and almost an order of magnitude cheaper) than field testing, but the acceleration and thermal characteristics of hydrodynamic generators are not the same as those of large caliber weapons. Therefore, field testing must be the final determining factor for establishing the suitability of a transducer, but it cannot be the sole form of testing used (see Section 7.2).

Ideally, we would have liked to see the development of this system through all stages of testing and improving of the transducers, including testing them in a gun chamber during weapon firing. However, the funding available for this Phase II project only allowed for preliminary laboratory testing of transducers at LIGHTWAVE and BRL; no provisions were made for field testing.

Initially, we were able to test the system thermally by monitoring the response of the transducer to temperature changes of the etalon. By cooling the transducer directly, we were able to produce a length contraction similar to that due to the pressure change, thereby

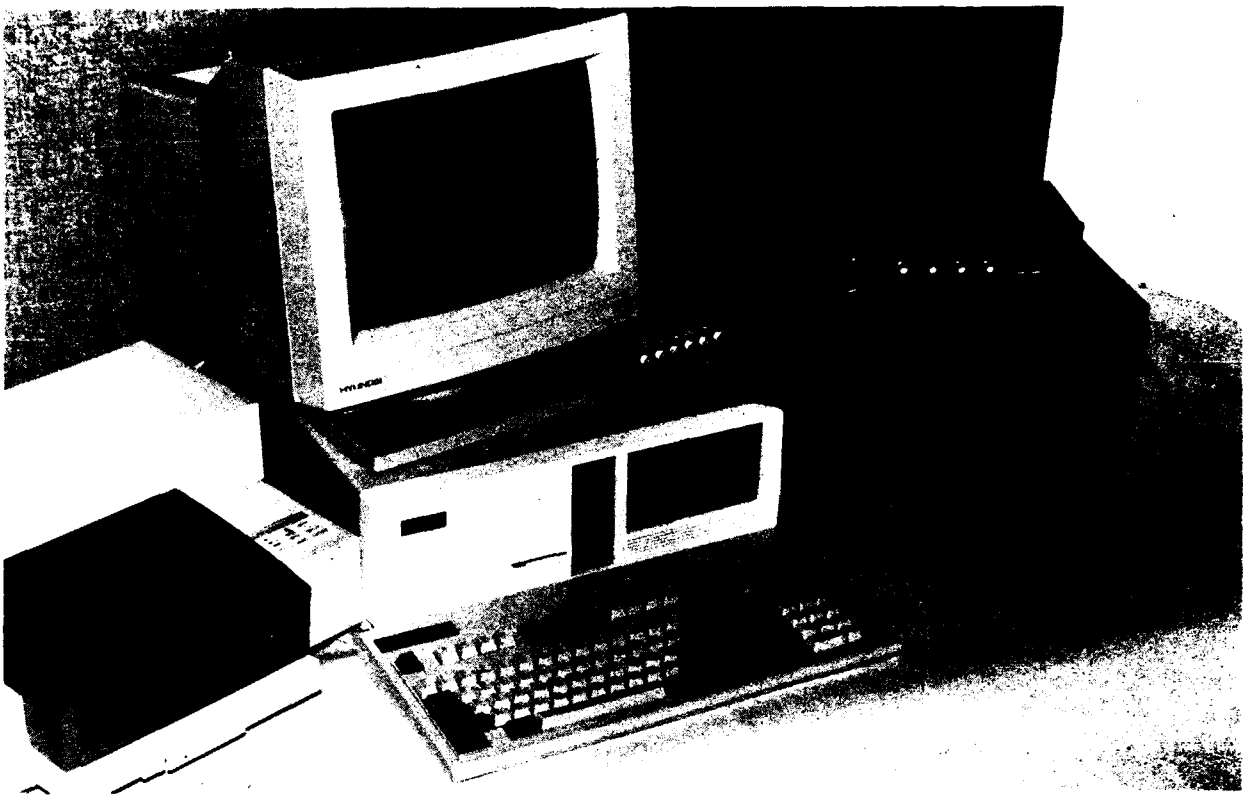

Figure 10. Photograph of the Whole System. The Black Box on the Right Contains the Laser, Fiber Coupler, and Detectors. The Interface Box Is Seen Just to the Left of the Black Box. On the Left Is the Personal Computer Controller and Printer.

simulating the optical response of the transducer to length changes induced by high pressures. This allowed the functionality of the system to be tested easily.

Limited high pressure testing was also performed in our laboratory at LIGHTWAVE using a Kistler hydrostatic high pressure generator that was obtained on loan from BRL. This equipment contains a small volume (2 cm^3) filled with a special oil that can be pressurized up to 105 psi simply by hand operation of crank handles. As described in Section 3.4, this high pressure generator was very useful for testing the pressure seal of the transducers. It was found that the seal could contain pressures up to 105 psi repeatably for extended periods. However, it was difficult to test the transducers dynamically using this hydrostatic pressure generator because there was no manner in which a rapid pressure change could be generated. It was possible to do quasistatic measurements, but the mechanical, hand-driven nature of the method used to change the pressure made this operationally difficult.

Using this approach, the response of the coated sapphire etalons as a function of pressure was measured. The reflected signal from the etalon was monitored as the pressure was varied, and a clear interference pattern was detected. Both polarization components were observed, and they were found to have a relative phase shift due to the birefringence of the sapphire, as necessary for determining the direction of the pressure change. One fringe shift was observed to correspond to a pressure change of 5,000 psi. This is in agreement with the fringe shift calculated by using the nominal values for the compressibility and the pressure dependence of the index of refraction of sapphire (see Section 1).

5.1 Testing at BRL. The compact, integrated prototype system was assembled and transported to BRL for an initial round of testing that was undertaken from 20–23 March 1990. The aim was to perform preliminary dynamic testing using a hydrodynamic pressure multiplier instrument to measure the response of a few test transducers to transient high pressure events which we had no means of producing at LIGHTWAVE. This provided a means to check that the transducers could withstand and contain dynamic pressure changes and to measure the response time of the transducers. Four fiber-coupled transducers were assembled for use in these tests. Three of them incorporated connectors between the coupling lens and the transducer, and the other one did not. The PC-based data acquisition system was not used in these tests since a fast transient digitizer was available at BRL. This device provided a means of logging detailed data on the response of the transducers, which could then be written onto a floppy disk and subsequently used in the development of the signal analysis routines for the PC data acquisition system. It was also hoped that we might be able to test a transducer in a less benevolent environment, such as a closed bomb test, to check its sensitivity to thermal effects.

The trip provided a good opportunity to meet with members of the BRL staff to discuss this project and obtain their input. Unfortunately, the testing of the system was hampered by an unexpected incompatibility between the optical transducer housing (based on the Kistler 6211 and the NATO standard metric package, which is widely used at Aberdeen) and the test ports on the equipment available at BRL for the testing, which were adapted for the use of the Kistler 607 (English style) pressure transducers. A fitting on the hydrodynamic high pressure multiplier system was modified for use with the Kistler 6211 transducer, allowing some tests to

be performed; but it was not possible to test a transducer in a closed bomb as had been hoped for.

A pressure transient was produced by opening a valve on the pressure multiplier system after it had been pressurized. Although the transient was not as fast as had been expected, it did allow the time response of the transducer to be monitored over a period of 200–300 ms. On this time scale, the transducer responded immediately to the pressure change, and clear interference fringes were visible while the pressure varied.

During the testing, the connectorized sensors were found to have larger levels of reflection from the connector interface than was previously observed at LIGHTWAVE. It proved to be impossible to reduce these reflections to an acceptable level during this testing period. This problem was not seen with the unconnectorized transducers, and the connectorized transducers operated fine when the connectors were removed, and the beam was coupled directly into them. Consequently, the use of connectors on the optical fiber was abandoned for the rest of the project period. This is an aspect that could receive further attention during subsequent development work.

The system was also found to be sensitive to vibrations, with local vibrational noise resulting in a noisy optical signal. This sensitivity was apparently due to variations in the coupling of the signal between the etalon and the single mode fiber, which is very sensitive to changes in angle between the fiber and SELFOC or between the SELFOC and etalon, so that it is possible for the transducer to act like a microphone. This vibrational sensitivity was not previously observed at LIGHTWAVE, presumably due to the vibrationally quiet environment in our laboratory. These problems were removed in the final versions of the transducer by mounting the optics more firmly and by using a suitable strain relief of the fiber cabling at the transducer end. Also, some of the final transducers were assembled using an alternative SELFOC lens (S2.0), which has a higher NA (0.37), so that the coupling is less sensitive to angular changes than with the SELFOC lens first used (N2.0, with NA = 0.16), although the S2.0 lens yields a slightly reduced coupling efficiency. Since the S2.0 lens is considerably shorter than the N2.0 lens (6.5 mm as compared to 16 mm), transducers incorporating this lens should also have a significantly higher stability towards mechanical vibrations because the shorter lens reduces the lever arm to the fiber end.

Shortly after this first visit to BRL, Dr. Richard Beyer arranged for two etalons mounted in transducer heads to be tested in the firing of a 105-mm Howitzer gun at APG. One transducer was mounted forward and the other at the rear in the gun chamber. No thermal protection over the exposed etalon (such as a layer of vacuum grease) was used. This was a basic test of the sapphire material to determine whether it was able to withstand the conditions in a gun chamber environment in the chosen mounting configuration. The pressure trace registered by an electronic (Kistler) gauge during this test is shown in Figure 11; the maximum pressure reached 70,000 psi. Both transducers maintained the pressure in chamber with evidently no loss of pressure seal. When they were removed from the gun chamber, they were both found to have carbon deposits on them. The one etalon survived the test completely intact with no visible damage to the sapphire, but there was damage to the outer reflective coating, although this may have been due to cleaning of the soot layer from the etalon during initial checking of its condition at BRL. However, the test generated two fine cracks in the other etalon.

The cracks were about 0.5 mm deep and very close to parallel for their whole length. One crack was across the middle of the face of the etalon, while the other was about 0.5 mm from the edge. It cannot be determined with certainty whether it was thermal shock or the high pressure pulse or indeed both that caused the cracks to appear. Poor seating of the etalon could also have played a role. However, we believe that these cracks resulted from the thermal shock experienced by the material during the firing of the gun, rather than as a result of the pressure applied to it. No thermal protection of the etalon surface was used in this test. We expect that if the pressure pulse caused failure of the bulk material, this would lead to cracks right though the etalon. Otherwise, if the cracks were only partially through the material, then we expect that they would be on the inner as opposed to the outer surface of the etalon.

Also, the maximum pressure generated in this event was not particularly high, and no cracks were ever observed during testing of the etalons at up to 100,000 psi in the hydrostatic generator. We discussed this with Mark Felt of Crystal Systems, Salem, MA, the suppliers of the sapphire that we used. He agreed that the observed failure of the sapphire was probably due to thermal shock. He noted that sapphire is susceptible to surface damage during fabrication that can lead to surface failures. This problem can be avoided if special care is taken during fabrication. Anyway, the final transducer design requires some form of thermal

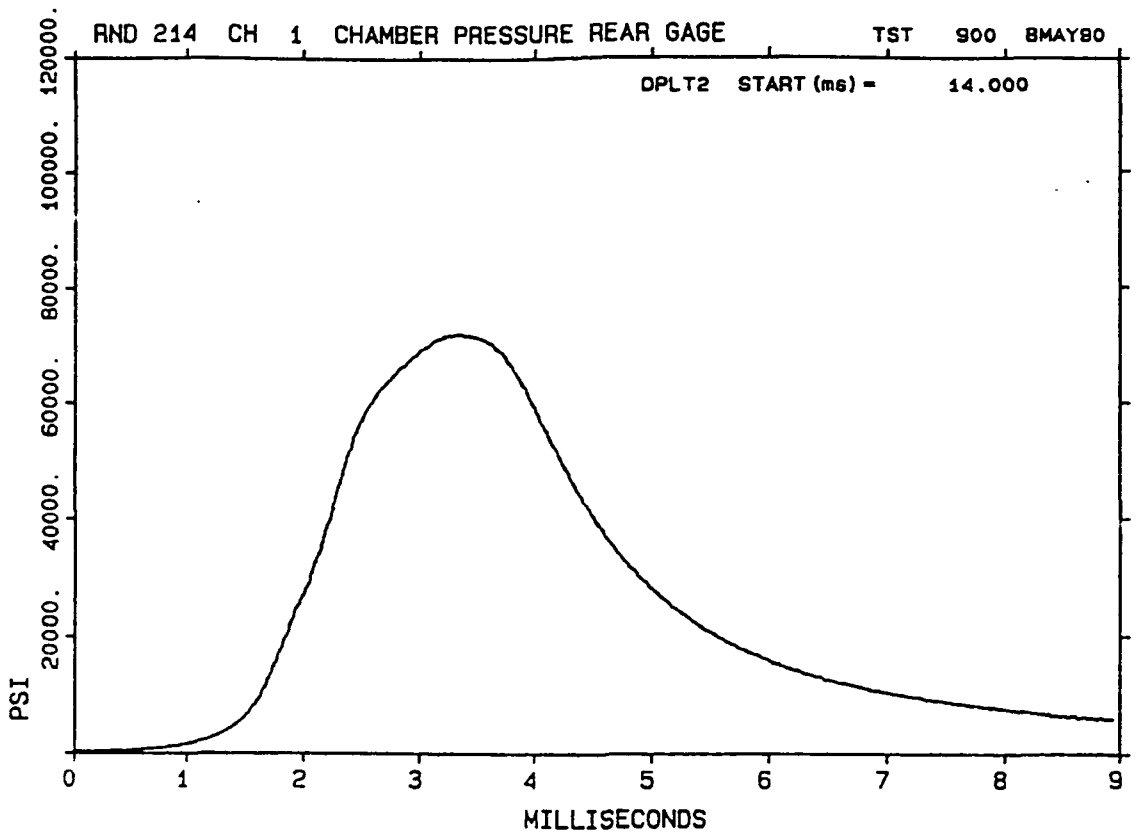

Figure 11. The Pressure Transient Generated by the Firing of a Howitzer Gun During Testing of Two Transducers.

insulating layer on top of the etalon, either an ablative layer (e.g., thermal grease) or else a durable crystalline cap, such as a 1- to 2-mm-thick sapphire or cubic zirconia layer. This will eliminate the possibility of damage to the transducer resulting from thermal shock.

The full prototype system was delivered to BRL during a second visit in July 1990, after completion of our research effort, to allow for more testing to be performed. Five transducers were assembled and delivered for these tests. Two of them incorporated the SELFOC lenses we used initially (N2.0), and the other three were based on the alternative, shorter SELFOC (S2.0). None of them included connectorized joints because of the problems we encountered with this approach previously; instead, each was supplied with a coupling lens permanently fixed to the input end. We demonstrated the use of the final version of the system, including operation of the data acquisition system implemented on the dedicated personal computer. Unfortunately, there was limited time available for testing during this visit. We checked for any extraneous microphonic vibrational noise pickup effects from the transducer, which had been seen during the previous trip to BRL, but none were observed. So apparently, the improved

arrangement for strain relief of the fiber cabling at the transducer end works correctly. The system was left at BRL for detailed testing and evaluation to be performed by personnel there. We look forward to receiving the results of this testing.

6. CONCLUSIONS

6.1 System Evaluation. We have investigated the various elements of the interferometric high pressure measurement system and have found that this approach to measuring high pressure transient events is indeed practicable. We assembled an integrated prototype pressure transient measurement system which has a sensitivity exceeding that required to meet the specifications listed in Section 3. The particular advantage that this approach offers is that it utilizes all-optical monitoring of the pressure, so that it is immune to electromagnetic interference. Of course, additional research and development that was outside the scope of this Phase II effort remains to be performed, and there are a number of aspects of the system which can be improved. In particular, more detailed testing and subsequent refinement of the transducers are required, and once field testing has been performed, appropriate custom PC-based signal analysis routines need to be written. This has not been done yet because no transducers have been tested in gun chambers; so no actual test data from the environment in which transducers are to be used is available on which to base the analysis. In particular, the level and type of system noise has not yet been quantified. Rather, we have concentrated on the optical aspects of the project in order to research them as fully as possible. Consequently, evaluation of the system cannot be conclusive at this stage.

The problem addressed by this measurement system is a difficult one, mostly because the transducers have to function in a particularly adverse environment. Exposure to gun chambers involves not only very high pressures, but also shock, vibration, and high temperature. It is the requirement that the small, delicate single mode fiber, which by its nature must entail sensitive optical coupling, has to function reliably in this extreme environment that is the main difficulty with practical realization of the approach used here. Also, this application requires that it is the reflected signal rather than the transmitted signal which has to be monitored, further complicating the implementation of this approach. To the best of our knowledge, previous attempts to measure high pressures optically for this kind of application have not been successful.

Unfortunately, the approach used in this measurement system has a number of inherent drawbacks. For instance, correct operation of the system requires time-consuming alignment of the laser polarization and the two photodetectors with respect to the initially unknown orientation of the etalon axes. It also necessitates involved data analysis of the pair of multivalued interference patterns in order to extract the pressure signal. In addition, it requires a sophisticated, optically isolated, narrow linewidth laser source and a dedicated personal computer-based data acquisition system, which make it a fairly costly solution.

There are also some potential sources of operational problems with the system which may interfere with its functioning. Principal amongst these is a noisy signal which can disturb the measurement as discussed in Section 4.5.2. While most of the possible sources of this noise have been eliminated during design and assembly of the system, one source that is difficult to handle is possible disturbance of the polarization state in the single mode fiber, which can disrupt the measurement. This may be the ultimate limiting factor for this system. Another issue is the durability of the transducers (i.e., whether they are capable of withstanding multiple measurements while maintaining good coupling of the signal).

We conclude that this interferometric measurement approach yields high sensitivity, but it requires a sophisticated system with fairly complex setup requirements and careful handling of the single mode fiber. Consequently, it should be suitable for use in measurements in a laboratory situation, but will probably not be appropriate for testing of guns in the field, where new rounds are fired approximately every two minutes. An alternative approach that we have proposed, which relies on an intensity-based scheme (see Section 6.3), would have lower sensitivity but would require a simpler system with direct signal readout and a more robust transducer design. We believe that such a system would be capable of handling the rigors and requirements of field testing.

6.2 Future Work. Now that a workable system configuration has been developed, we are interested in performing further development work to optimize it and to perform detailed transducer testing. Obviously, a good deal has been learned during this initial research and development effort, and we are now set for much more rapid progress.

As described previously, room remains for improvement. The main aspect that needs to be attacked is further detailed testing, evaluation, and optimization of the transducers, in order

to quantify their performance and achieve maximum robustness. This will require testing not only in the laboratory but also in the field. These results can then be used in developing specific computer routines for automated analysis of the transducer signals. Another aspect which can be further investigated is the use of a connectorized joint on the fiber between the coupling lens and the transducer to allow for easier operation.

Although LIGHTWAVE Electronics has a strong program of contract research and has been awarded numerous SBIR research contracts, it is primarily a product-oriented company. LIGHTWAVE has been very successful in developing commercial products based on the results of SBIR research, which is one of the major aims of the SBIR program. If the unresolved issues with the current system that have been described previously can be eliminated or reduced, and if there is sufficient military or commercial interest in this measurement system, LIGHTWAVE will pursue commercialization of it. The obvious immediate application of this system would be in the current Army program to develop and evaluate electrothermal guns. This system would be of immediate use in that effort. In particular, the immunity of this system to electromagnetic interference is of particular importance in the testing of electrothermal guns due to the intense electromagnetic pulse produced when these guns are fired.

There are also other research applications for this system. For instance, David Benson at Sandia National Laboratories, Albuquerque, NM, is interested in using such a system for measuring the pressure rise due to the arc produced when a very high current (100 kAmp) electric discharge is turned on. Measurements in this environment are also plagued by problems due to electromagnetic interference. These events occur on a shorter time scale (event duration of 100 μs) and involve higher instantaneous temperatures than in a gun chamber during weapon firing. Consequently, some adaptation of the current system would be necessary, notably the data acquisition system would have to be faster, and the transducers would require careful thermal protection. However, they are currently set up for the use of Kistler gauges so a transducer similar to the one we have developed would already be compatible with their equipment.

This optical high pressure measurement system may have commercial applications, since high pressures need to be monitored in many industrial situations. Being compact, minimally

intrusive, having a wide range, good sensitivity and fast response, while requiring low power and being immune to electromagnetic interference, this system offers many advantages over currently available technology. The technique used here may also be easily adaptable to lower pressure ranges by utilizing other transducer materials that are more elastic (e.g., lucite, or other optically clear plastics).

6.3 Alternative Approach. We have recently submitted a new SBIR Phase I proposal to investigate the feasibility of an alternative approach to obtaining an optical high pressure transient measurement system, which would be intensity based rather than interferometric in nature. This proposed approach applies the concept of a "fiber optic lever" to arrive at a simple intensity-based measurement system. It would utilize a multimode fiber bundle to illuminate and collect a reflected signal from a durable optical crystal transducer that would be very similar to the etalon used in the above approach. A high intensity light emitting diode (LED) or a laser diode would suffice as the source of optical power in this case. Since the collected optical signal would depend monotonically on the pressure applied to the transducer, it would generate an output signal that would depend directly on the applied pressure. Thus, this approach would not require a complex data acquisition and analysis system or a sophisticated, costly laser source. It would also avoid using delicate single mode fiber with the attendant sensitive fiber coupling; the multimode fiber would have a large-core diameter (say 0.5 mm) and so would be easier to handle and have a less sensitive coupling than single mode fiber. This system would also not be subject to interferometric noise, and the transducer is expected to be more robust. However, it would have lower sensitivity than the interferometric transducer developed here, and would require low system intensity noise. While the current program and the new proposed research have essentially the same aims, the approaches are substantially different (viz., a sophisticated interferometric approach vs. a simplified intensity approach).

While the interferometric system described previously can provide adequate performance, we believe that the new proposal will lead to a system with the required performance that is simpler and less costly. It incorporates the best elements of the interferometric system we have previously studied, but is simpler in design and would be considerably easier to use. Also, the experience we have accumulated during our research effort to date lends confidence to our belief that the new pressure measurement system we have proposed should indeed be feasible. We look forward to the possibility of investigating this alternative approach.

7. OPERATING INSTRUCTIONS

7.1 System Setup. The box containing the laser source, fiber coupler, and detector assembly must be located close enough to the measurement point so that the fiber attached to the transducer reaches back to the source. The personal computer controller can be located further away, with sufficiently long cables connecting the signal outputs to the input ports for the A/D board. The various components must be connected as follows. The two cords supplying power to the laser and detectors must be plugged into the matching connectors on the back panel of the laser power supply. The P and S signal outputs must be connected via BNC cables to the channel 0 and 1 inputs (labelled P and S) on the blue interface box. The ribbon cable out of this blue box should already be connected to the input terminal on the back of the DAS-50 board, which is installed in the main PC chassis. The trigger input cable must be connected to the digital trigger (DGTL TRG) connector on the blue interface box. This assumes the trigger is a TTL compatible signal, which should be produced immediately prior to the high pressure transient event to be measured.

When the laser is turned on, it takes a few minutes (3–5) for the temperature of the system to stabilize, during which time no beam is emitted. Once the beam is visible, the laser and measurement system are ready for use.

7.2 Operation of the System.

- Initial transducer head installation.
  - (1) The laser beam must be coupled into the optical fiber attached to the transducer head while monitoring the intensity of the light transmitted through the transducer. The coupling must be optimized by adjusting the angles and lateral position of the coupling lens held in the fiber coupling mount so as to maximize the transmitted signal. It may be necessary to adjust the laser frequency to ensure that the etalon is close to a transmitted interference maximum.
  - (2) The fiber coupling lens must then be removed from the coupler by loosening the set screw, noting the original position of the lens.
  - (3) A layer of vacuum grease (e.g., Apiezon N) must be applied to the exposed surface of the etalon transducer, filling the 1-mm depression. This acts as an

ablative layer that insulates the etalon from the immediate effects of the temperature rise when the weapon is fired. The transducer head must then be carefully mounted in position in the test port, trying to minimize twisting of the cable.

(4) The coupling lens must then be replaced in the fiber coupling mount in its original position, and the set screw must be retightened.

(5) The coupling must be remaximized by monitoring the reflected signal observed out of the beam splitter at the input end of the fiber. Only a small amount of angular adjustment should be necessary. It may be necessary to adjust the laser frequency to ensure that the etalon is close to a reflected interference maximum. The signal level should be at least 100–200 μW at the interference peak.

- Polarization alignment.

The laser polarization must be aligned midway between the two etalon axes as follows:

(6) The P and S signals must be monitored separately using two voltmeters while varying the orientations of the half-wave plate and analyzing beam splitter in order to minimize the S-signal.

(7) The correct positions are attained when the S-signal remains minimal even when the laser frequency is scanned, and the P-signal is a clear single etalon pattern vs. frequency. Use the "SCAN" program to measure the etalon patterns as a function of frequency, invoke PC Data Master (by typing "DM"), convert the data file from SCAN to binary form (using "ATOB <input_file> <output_file>"), and plot the results using the "PLOT" command.

(8) Small adjustments of the half-wave plate and analyzing beam splitter may be necessary to obtain the best alignment. This position aligns the laser polarization parallel to one axis of the etalon and aligns the analyzing beam splitter with respect to the two etalon axes.

(9) The half-wave plate must then be rotated (either direction) by 22.5° (rotating the laser polarization by 45°) to set the polarization in the required position midway between the etalon axes.

- Prepare the data acquisition system and perform the measurement of the high pressure event.
  (10) Type "ACQUIRE" to obtain the default setup of the data acquisition. The parameters will be set to their default values, and then a control panel will be shown displaying these values, which should then be checked. If any of the defaults are not appropriate (e.g., digitization rate or number of data points), then they can be reset using the control panel.
  (11) In general, a TTL trigger just prior to the event should be applied to the DGTL TRG port in order to trigger the logging of the data. Alternative trigger modes can be selected if desired (see the DAS-50 Manual for further details).
  (12) The message "BUSY" will flash in the top right hand corner of the control panel while awaiting the trigger signal, and the "Buffer Trig Addr" in the bottom left hand corner will be "********".
  (13) Once the trigger has been received, the "Buffer Trig Addr" will display "0000000". When all the data have been logged, the control panel will automatically be hidden.
  (14) After the event has been measured, the first 32,000 data points (i.e., 16,000 points per channel) can be logged immediately to a data file D:\<filename>.DAT, with <filename> specified by the user.

- Saving alternative data files after the measurement.
  (15) Type "STORE" to transfer data from the DAS-50 local memory to a file on the \D: drive. The user will be prompted for a file name. This routine allows 32,000 points per channel to be logged to separate data files (avoiding the 16,000 point limit in ACQUIRE). It also allows different sections of the data to be logged, instead of just the first section.
  (16) Note that the DAS-50 local memory is volatile, so the data will be lost should the PC lose power or be rebooted. Consequently, the data should be stored on the hard disk as soon as possible.

- Analyze the data.
  (17) Type "ANALYZE" to display and analyze data stored on the \D: drive. This launches PC Data Master; use <enter> to display the console. A set of

commands is available for plotting the data and analyzing the pressure response (see the PC Data Master Manual for further details.)

(18) Note that the data files are written to the hard disk by the programs; "ACQUIRE" and "STORE" are written in ASCII format. This allows them to be easily examined using a text editor. In order to plot the data using PC Data Master, they must first be converted to a binary format by using the Data Master command "ATOB <ascii_input_file> <binary_output_file>". The binary file is also more compact than the ASCII file, so it should be the form used for long-term data storage.

8. REFERENCES

Born, M., and E. Wolf. Principles of Optics. 5th ed., Oxford: Pergamon Press, 1975.

Crystal Systems Inc. HEM Sapphire Brochure. Salem, MA, 1990.

Giallorenzi, T. G., et al. "Optical Fiber Sensor Technology." IEEE J. Quant. Elect., vol. QE-18, p. 626, 1982.

Gray, D. E. (ed.). American Institute of Physics Handbook. 3rd ed., New York: McGraw-Hill, 1982.

Kane, T. J., and R. L. Byer. "A Monolithic, Unidirectional Single-Mode Nd:YAG Ring Laser." Opt. Lett., vol. 10, p. 65, 1985.

Kersey, A. D., T. G. Giallorenzi, and A. Dandridge. "Interferometric and Intensity Sensors Become More Sophisticated." Laser Focus World, p. 137, July 1989.

Melles Griot Corp. Melles Griot Optics Guide 4. Irvine, CA, p. 3–14, 1988.

Pinnow, D. A. "Guidelines for Selection of Acousto-Optic Materials." IEEE J. Quant. Elect., vol. QE-6, p. 223, 1970.

Schmitt, R. L., and L. A. Rahn. "Diode-Laser-Pumped Nd:YAG Laser Injection Seeding System." Appl. Opt., vol. 25, p. 629, 1986.

Walton, W. S. "Weapon Chamber Pressure Measurement." Proceedings of the 12th Transducer Workshop, Melbourne, FL, pp. 256–281, June 1983. (AD-A137304)

Zhou, B., T. J. Kane, G. J. Dixon, and R. L. Byer. "Efficient, Frequency-Stable Laser Diode Pumped Nd:YAG Laser." Opt. Lett., vol. 10, p. 62, 1985.

INTENTIONALLY LEFT BLANK.

No. of Copies	Organization
2	Administrator Defense Technical Info Center ATTN: DTIC-DDA Cameron Station Alexandria, VA 22304-6145
1	Commander U.S. Army Materiel Command ATTN: AMCAM 5001 Eisenhower Avenue Alexandria, VA 22333-0001
1	Commander U.S. Army Laboratory Command ATTN: AMSLC-DL 2800 Powder Mill Road Adelphi, MD 20783-1145
2	Commander U.S. Army Armament Research, Development, and Engineering Center ATTN: SMCAR-IMI-I Picatinny Arsenal, NJ 07806-5000
2	Commander U.S. Army Armament Research, Development, and Engineering Center ATTN: SMCAR-TDC Picatinny Arsenal, NJ 07806-5000
1	Director Benet Weapons Laboratory U.S. Army Armament Research, Development, and Engineering Center ATTN: SMCAR-CCB-TL Watervliet, NY 12189-4050
(Unclass. only)1	Commander U.S. Army Armament, Munitions and Chemical Command ATTN: AMSMC-IMF-L Rock Island, IL 61299-5000
1	Director U.S. Army Aviation Research and Technology Activity ATTN: SAVRT-R (Library) M/S 219-3 Ames Research Center Moffett Field, CA 94035-1000

No. of Copies	Organization
1	Commander U.S. Army Missile Command ATTN: AMSMI-RD-CS-R (DOC) Redstone Arsenal, AL 35898-5010
1	Commander U.S. Army Tank-Automotive Command ATTN: ASQNC-TAC-DIT (Technical Information Center) Warren, MI 48397-5000
1	Director U.S. Army TRADOC Analysis Command ATTN: ATRC-WSR White Sands Missile Range, NM 88002-5502
1	Commandant U.S. Army Field Artillery School ATTN: ATSF-CSI Ft. Sill, OK 73503-5000
(Class. only)1	Commandant U.S. Army Infantry School ATTN: ATSH-CD (Security Mgr.) Fort Benning, GA 31905-5660
(Unclass. only)1	Commandant U.S. Army Infantry School ATTN: ATSH-CD-CSO-OR Fort Benning, GA 31905-5660
1	Air Force Armament Laboratory ATTN: WL/MNOI Eglin AFB, FL 32542-5000
	Aberdeen Proving Ground
2	Dir, USAMSAA ATTN: AMXSY-D AMXSY-MP, H. Cohen
1	Cdr, USATECOM ATTN: AMSTE-TC
3	Cdr, CRDEC, AMCCOM ATTN: SMCCR-RSP-A SMCCR-MU SMCCR-MSI
1	Dir, VLAMO ATTN: AMSLC-VL-D
10	Dir, BRL ATTN: SLCBR-DD-T

No. of Copies | Organization

1 HQDA (SARD-TC, C.H. Church)
WASH DC 20310-0103

4 Commander
US Army Research Office
ATTN: R. Ghirardelli
D. Mann
R. Singleton
R. Shaw
P.O. Box 12211
Research Triangle Park, NC
27709-2211

2 Commander
US Army Armament Research,
Development, and Engineering Center
ATTN: SMCAR-AEE-B, D.S. Downs
SMCAR-AEE, J.A. Lannon
Picatinny Arsenal, NJ 07806-5000

1 Commander
US Army Armament Research,
Development, and Engineering Center
ATTN: SMCAR-AEE-BR, L. Harris
Picatinny Arsenal, NJ 07806-5000

2 Commander
US Army Missile Command
ATTN: AMSMI-RD-PR-E, A.R. Maykut
AMSMI-RD-PR-P, R. Betts
Redstone Arsenal, AL 35898-5249

1 Office of Naval Research
Department of the Navy
ATTN: R.S. Miller, Code 432
800 N. Quincy Street
Arlington, VA 22217

1 Commander
Naval Air Systems Command
ATTN: J. Ramnarace, AIR-54111C
Washington, DC 20360

1 Commander
Naval Surface Warfare Center
ATTN: J.L. East, Jr., G-23
Dahlgren, VA 22448-5000

No. of Copies | Organization

2 Commander
Naval Surface Warfare Center
ATTN: R. Bernecker, R-13
G.B. Wilmot, R-16
Silver Spring, MD 20903-5000

5 Commander
Naval Research Laboratory
ATTN: M.C. Lin
J. McDonald
E. Oran
J. Shnur
R.J. Doyle, Code 6110
Washington, DC 20375

1 Commanding Officer
Naval Underwater Systems
Center Weapons Dept.
ATTN: R.S. Lazar/Code 36301
Newport, RI 02840

2 Commander
Naval Weapons Center
ATTN: T. Boggs, Code 388
T. Parr, Code 3895
China Lake, CA 93555-6001

1 Superintendent
Naval Postgraduate School
Dept. of Aeronautics
ATTN: D.W. Netzer
Monterey, CA 93940

3 AL/LSCF
ATTN: R. Corley
R. Geisler
J. Levine
Edwards AFB, CA 93523-5000

1 AFOSR
ATTN: J.M. Tishkoff
Bolling Air Force Base
Washington, DC 20332

1 OSD/SDIO/IST
ATTN: L. Caveny
Pentagon
Washington, DC 20301-7100

No. of Copies	Organization
1	Commandant USAFAS ATTN: ATSF-TSM-CN Fort Sill, OK 73503-5600
1	F.J. Seiler ATTN: S.A. Shackleford USAF Academy, CO 80840-6528
1	University of Dayton Research Institute ATTN: D. Campbell AL/PAP Edwards AFB, CA 93523
1	NASA Langley Research Center Langley Station ATTN: G.B. Northam/MS 168 Hampton, VA 23365
4	National Bureau of Standards ATTN: J. Hastie M. Jacox T. Kashiwagi H. Semerjian US Department of Commerce Washington, DC 20234
1	Aerojet Solid Propulsion Co. ATTN: P. Micheli Sacramento, GA 95813
1	Applied Combustion Technology, Inc. ATTN: A.M. Varney P.O. Box 607885 Orlando, FL 32860
2	Applied Mechanics Reviews The American Society of Mechanical Engineers ATTN: R.E. White A.B. Wenzel 345 E. 47th Street New York, NY 10017
1	Atlantic Research Corp. ATTN: M.K. King 5390 Cherokee Avenue Alexandria, VA 22314

No. of Copies	Organization
1	Atlantic Research Corp. ATTN: R.H.W. Waesche 7511 Wellington Road Gainesville, VA 22065
1	AVCO Everett Research Laboratory Division ATTN: D. Stickler 2385 Revere Beach Parkway Everett, MA 02149
1	Battelle ATTN: TACTEC Library, J. Huggins 505 King Avenue Columbus, OH 43201-2693
1	Cohen Professional Services ATTN: N.S. Cohen 141 Channing Street Redlands, CA 92373
1	Exxon Research & Eng. Co. ATTN: A. Dean Route 22E Annandale, NJ 08801
1	General Applied Science Laboratories, Inc. 77 Raynor Avenue Ronkonkama, NY 11779-6649
1	General Electric Ordnance Systems ATTN: J. Mandzy 100 Plastics Avenue Pittsfield, MA 01203
1	General Motors Rsch Labs Physical Chemistry Department ATTN: T. Sloane Warren, MI 48090-9055
2	Hercules, Inc. Allegheny Ballistics Lab. ATTN: W.B. Walkup E.A. Yount P.O. Box 210 Rocket Center, WV 26726

No. of Copies | Organization

1 Alliant Techsystems, Inc.
Marine Systems Group
ATTN: D.E. Broden/
MS MN50-2000
600 2nd Street NE
Hopkins, MN 55343

1 Alliant Techsystems, Inc.
ATTN: R.E. Tompkins
MN38-3300
5700 Smetana Drive
Minnetonka, MN 55343

1 IBM Corporation
ATTN: A.C. Tam
Research Division
5600 Cottle Road
San Jose, CA 95193

1 IIT Research Institute
ATTN: R.F. Remaly
10 West 35th Street
Chicago, IL 60616

2 Director
Lawrence Livermore
National Laboratory
ATTN: C. Westbrook
M. Costantino
P.O. Box 808
Livermore, CA 94550

1 Lockheed Missiles & Space Co.
ATTN: George Lo
3251 Hanover Street
Dept. 52-35/B204/2
Palo Alto, CA 94304

1 Director
Los Alamos National Lab
ATTN: B. Nichols, T7, MS-B284
P.O. Box 1663
Los Alamos, NM 87545

1 National Science Foundation
ATTN: A.B. Harvey
Washington, DC 20550

1 Olin Ordnance
ATTN: V. McDonald, Library
P.O. Box 222
St. Marks, FL 32355-0222

No. of Copies | Organization

1 Paul Gough Associates, Inc.
ATTN: P.S. Gough
1048 South Street
Portsmouth, NH 03801-5423

2 Princeton Combustion
Research Laboratories, Inc.
ATTN: M. Summerfield
N.A. Messina
475 US Highway One
Monmouth Junction, NJ 08852

1 Hughes Aircraft Company
ATTN: T.E. Ward
8433 Fallbrook Avenue
Canoga Park, CA 91303

1 Rockwell International Corp.
Rocketdyne Division
ATTN: J.E. Flanagan/HB02
6633 Canoga Avenue
Canoga Park, CA 91304

4 Director
Sandia National Laboratories
Division 8354
ATTN: R. Cattolica
S. Johnston
P. Mattern
D. Stephenson
Livermore, CA 94550

1 Science Applications, Inc.
ATTN: R.B. Edelman
23146 Cumorah Crest
Woodland Hills, CA 91364

3 SRI International
ATTN: G. Smith
D. Crosley
D. Golden
333 Ravenswood Avenue
Menlo Park, CA 94025

1 Stevens Institute of Tech.
Davidson Laboratory
ATTN: R. McAlevy, III
Hoboken, NJ 07030

No. of Copies | Organization

1 Sverdrup Technology, Inc.
LERC Group
ATTN: R.J. Locke, MS SVR-2
2001 Aerospace Parkway
Brook Park, OH 44142

1 Sverdrup Technology, Inc.
ATTN: J. Deur
2001 Aerospace Parkway
Brook Park, OH 44142

1 Thiokol Corporation
Elkton Division
ATTN: S.F. Palopoli
P.O. Box 241
Elkton, MD 21921

3 Thiokol Corporation
Wasatch Division
ATTN: S.J. Bennett
P.O. Box 524
Brigham City, UT 84302

1 United Technologies Research Center
ATTN: A.C. Eckbreth
East Hartford, CT 06108

3 United Technologies Corp.
Chemical Systems Division
ATTN: R.S. Brown
T.D. Myers (2 copies)
P.O. Box 49028
San Jose, CA 95161-9028

1 Universal Propulsion Company
ATTN: H.J. McSpadden
Black Canyon Stage 1
Box 1140
Phoenix, AZ 85029

1 Veritay Technology, Inc.
ATTN: E.B. Fisher
4845 Millersport Highway
P.O. Box 305
East Amherst, NY 14051-0305

1 Brigham Young University
Dept. of Chemical Engineering
ATTN: M.W. Beckstead
Provo, UT 84058

No. of Copies | Organization

1 California Institute of Tech.
Jet Propulsion Laboratory
ATTN: L. Strand/MS 512/102
4800 Oak Grove Drive
Pasadena, CA 91109

1 California Institute of Technology
ATTN: F.E.C. Culick/MC 301-46
204 Karman Lab.
Pasadena, CA 91125

1 University of California
Los Alamos Scientific Lab.
P.O. Box 1663, Mail Stop B216
Los Alamos, NM 87545

1 University of California, Berkeley
Chemistry Deparment
ATTN: C. Bradley Moore
211 Lewis Hall
Berkeley, CA 94720

1 University of California, San Diego
ATTN: F.A. Williams
AMES, B010
La Jolla, CA 92093

2 University of California, Santa Barbara
Quantum Institute
ATTN: K. Schofield
M. Steinberg
Santa Barbara, CA 93106

1 University of Colorado at Boulder
Engineering Center
ATTN: J. Daily
Campus Box 427
Boulder, CO 80309-0427

2 University of Southern California
Dept. of Chemistry
ATTN: S. Benson
C. Wittig
Los Angeles, CA 90007

No. of Copies | Organization

1 Cornell University
Department of Chemistry
ATTN: T.A. Cool
Baker Laboratory
Ithaca, NY 14853

1 University of Delaware
ATTN: T. Brill
Chemistry Department
Newark, DE 19711

1 University of Florida
Dept. of Chemistry
ATTN: J. Winefordner
Gainesville, FL 32611

3 Georgia Institute of Technology
School of Aerospace Engineering
ATTN: E. Price
W.C. Strahle
B.T. Zinn
Atlanta, GA 30332

1 University of Illinois
Dept. of Mech. Eng.
ATTN: H. Krier
144MEB, 1206 W. Green St.
Urbana, IL 61801

1 Johns Hopkins University/APL
Chemical Propulsion
Information Agency
ATTN: T.W. Christian
Johns Hopkins Road
Laurel, MD 20707

1 University of Michigan
Gas Dynamics Lab
Aerospace Engineering Bldg.
ATTN: G.M. Faeth
Ann Arbor, MI 48109-2140

1 University of Minnesota
Dept. of Mechanical
Engineering
ATTN: E. Fletcher
Minneapolis, MN 55455

No. of Copies | Organization

3 Pennsylvania State University
Applied Research Laboratory
ATTN: K.K. Kuo
H. Palmer
M. Micci
University Park, PA 16802

1 Pennsylvania State University
Dept. of Mechanical Engineering
ATTN: V. Yang
University Park, PA 16802

1 Polytechnic Institute of NY
Graduate Center
ATTN: S. Lederman
Route 110
Farmingdale, NY 11735

2 Princeton University
Forrestal Campus Library
ATTN: K. Brezinsky
I. Glassman
P.O. Box 710
Princeton, NJ 08540

1 Purdue University
School of Aeronautics
and Astronautics
ATTN: J.R. Osborn
Grissom Hall
West Lafayette, IN 47906

1 Purdue University
Department of Chemistry
ATTN: E. Grant
West Lafayette, IN 47906

2 Purdue University
School of Mechanical
Engineering
ATTN: N.M. Laurendeau
S.N.B. Murthy
TSPC Chaffee Hall
West Lafayette, IN 47906

1 Rensselaer Polytechnic Inst.
Dept. of Chemical Engineering
ATTN: A. Fontijn
Troy, NY 12181

No. of Copies	Organization
1	Stanford University Dept. of Mechanical Engineering ATTN: R. Hanson Stanford, CA 94305
1	University of Texas Dept. of Chemistry ATTN: W. Gardiner Austin, TX 78712
1	University of Utah Dept. of Chemical Engineering ATTN: G. Flandro Salt Lake City, UT 84112
1	Virginia Polytechnic Institute and State University ATTN: J.A. Schetz Blacksburg, VA 24061
1	Freedman Associates ATTN: E. Freedman 2411 Diana Road Baltimore, MD 21209-1525

INTENTIONALLY LEFT BLANK.

USER EVALUATION SHEET/CHANGE OF ADDRESS

This laboratory undertakes a continuing effort to improve the quality of the reports it publishes. Your comments/answers below will aid us in our efforts.

1. Does this report satisfy a need? (Comment on purpose, related project, or other area of interest for which the report will be used.) _____

2. How, specifically, is the report being used? (Information source, design data, procedure, source of ideas, etc.) _____

3. Has the information in this report led to any quantitative savings as far as man-hours or dollars saved, operating costs avoided, or efficiencies achieved, etc? If so, please elaborate. _____

4. General Comments. What do you think should be changed to improve future reports? (Indicate changes to organization, technical content, format, etc.) _____

BRL Report Number BRL-CR-681 Division Symbol _____

Check here if desire to be removed from distribution list. ____

Check here for address change. ____

Current address: Organization _____
Address _____

DEPARTMENT OF THE ARMY
Director
U.S. Army Ballistic Research Laboratory
ATTN: SLCBR-DD-T
Aberdeen Proving Ground, MD 21005-5066

OFFICIAL BUSINESS

BUSINESS REPLY MAIL
FIRST CLASS PERMIT No 0001, APG, MD

Postage will be paid by addressee

Director
U.S. Army Ballistic Research Laboratory
ATTN: SLCBR-DD-T
Aberdeen Proving Ground, MD 21005-5066

NO POSTAGE
NECESSARY
IF MAILED
IN THE
UNITED STATES